

IFESIS: Instantaneous Frequencies Estimation via Subspace Invariance properties of wavelet Structures

Ioannis A. Antoniadis¹, Christos T. Yiakopoulos, Konstantinos C. Gryllias, Konstantinos I. Rodopoulos

Dynamics and Structures Laboratory, Machine Design and Control Systems Section,
School of Mechanical Engineering, National Technical University of Athens, Greece.

e-mail: ¹antogian@central.ntua.gr

Abstract

According to the proposed method, a set of wavelet transforms of the signal is first obtained, using a structure of Complex Shifted Morlet Wavelets. No specific constraints are imposed on the center frequencies and the bandwidths of the individual wavelets, as well as on the number of wavelets used. In this way, a set of complex signals result in the time domain, equal to the number of the wavelets used. Then, the instantaneous frequencies of the signals are estimated by applying an appropriate subspace algorithm (as for e.g. ESPRIT), to the entire set of the resulting complex wavelet transforms, exploiting the corresponding subspace rotational invariance property of this set of complex signals. Since the method proposes the application of the subspace algorithm after the signal has been appropriately transformed by an appropriate wavelet structure, contrary to the classical subspace methods which are applied to the signal itself, the desired time-frequency features of the signal are enhanced, while simultaneously, the undesired frequency components, as well as the noise, are suppressed. In this way, the method combines the advantages of the Complex Shifted Morlet Wavelets with the advantages of subspace based approaches. Moreover, the method provides a means for estimating the number of the resulting harmonic components, using as a relevant indicator the number of the non-zero singular values of the corresponding singular value decomposition problem. It should be noted that the resulting singular values are also time dependent, providing valuable information on the possibly time variable dynamic structure of the signal.

Keywords: Instantaneous frequency, Complex Shifted Morlet Wavelets, Subspace methods, eigenspace methods, rotational invariance.

1. Introduction

The estimation of the instantaneous frequency content of non-stationary multicomponent harmonic signals is of paramount importance in all signal processing applications of mechanical systems, including condition and health monitoring, operational modal analysis or even real time control. Equally important is such a need also in the broad range of signal processing applications, including for e.g. communications, speech and image processing, biomedical and environmental signal analysis, etc.

For this reason, this task has been addressed long ago. Boashash [1], [2] contributed an interpretation of the IF concept as well as a comprehensive review of the literature about IF estimation methods. In general, the IF estimation methods can be classified into five main categories: (a) phase difference-based IF estimators; (b) zero-crossing IF estimators; (c) linear-prediction-filter-based adaptive IF estimators; (d) IF estimators based on the moments of time–frequency distributions (TFDs); and (e) IF estimators based on the peak of TFDs. An indicative brief review of relevant approaches can be found among others in [3], [4]. Of special importance and effectiveness are methods based on single component variants of subspace based approaches, due to their enhanced resolution and robustness to noise. Moreover, among the TFD methods, far more interesting are IF estimations based on the Wavelet Transform [4], due to the established overall advantages of the Wavelet Transform over the other TFD methods.

Parallel, during the same time period, significant achievements have been accomplished in the field of parameter estimation of multicomponent harmonic signals. Among others, some indicative well-known milestone contributions in the field include all variants of subspace based approaches such as MUSIC [5], ESPRIT [6] and minimum norm [7], matching pursuit algorithms based on wavelet dictionaries [8], multiband variants of the well-known Energy Operator Separation Algorithm (EOSA) [9], Periodic algebraic separation and energy demodulation (PASED) [10], etc. Other general purpose approaches can be also used for the same purpose, such as Autoregressive Moving Average (ARMA) approaches [11], [12], Empirical Mode Decomposition [13] or appropriate extensions of the Hilbert Transform [14], [15].

Although a vast number and variety of relevant methods have been proposed, some key problems of such methods still exist. As it has been demonstrated for e.g. in [3], oversampling in relation to noise may lead to significant errors, even in the case of well established procedures. Therefore, the sampling frequency must be selected appropriately in relation to the noise level and the frequency content of the signal, which is a cumbersome task in the case of broadband signals. Moreover, if a signal containing multiple harmonics is interpreted as a single component signal, characteristic spikes appear in the time waveform of the instantaneous frequency, which resemble “outliers” or “impulsive noise” and consequently, they are often

misinterpreted as such. The real nature of this phenomenon can be only understood by a careful analysis of the analytical form of the instantaneous frequencies of signals including multiple harmonic components, as for e.g. those presented in Appendix A of [16], or more analytically in [17]. Thus, although a number of post processing procedures have been proposed [2] for smoothing the waveform of the instantaneous frequency, the effects of this phenomenon can be only mitigated but not alleviated.

Consequently, the problem of multiple instantaneous frequency estimation is closely related to the problem of the proper estimation and interpretation of the number of harmonic contained in a signal, a task which by itself is far from being trivial. Not only a variety of methods exist for estimating the number of harmonic components in a signal, but also the answer may differ according to the decomposition approach selected [18], [19]. Moreover, as it will be shown in this paper, the answer to this question may time dependent, as it should be anticipated in time variable systems.

In this paper, a method for multicomponent instantaneous frequency estimation is proposed, combining the advantages of the Complex Shifted Morlet Wavelets with the advantages of subspace based approaches. As summarized elsewhere [4], Complex Shifted Morlet Wavelets (CSMW) combine a number of advantages. First, since Morlet Wavelets are modulated in the time domain by a Gaussian shaped time window (and for this reason are also known as Gabor wavelets), they present the optimal resolution simultaneously in the time and in the frequency domain. Second, compared to the Discrete Wavelet Transform (DWT), they allow for the continuous (and thus more accurate) approximation in both time and frequency domains. Additionally, they are not related to spectral leakage effects. Third, contrary to the traditional real number representation of the Morlet Wavelet Transform, CSMW results to complex wavelet coefficients in the time domain, thus enabling the direct simultaneous calculation of the signal instantaneous amplitude and frequency. Fourth, contrary to the classical concept of “scaling” the wavelet in the time or frequency domain, which allows the identification of only just one parameter, -the wavelet scale- the concept of shifting the Morlet wavelet in the frequency domain allows for the simultaneous optimal selection of both the wavelet parameters necessary to identify it as a proper filter in the frequency domain: The center frequency and the bandwidth.

Finally, as it is shown in [4], the recovery of the signal frequency can be performed accurately, without the requirement that the wavelet center frequency coincides to the signal frequency, contrary to the accurate recovery of the signal amplitude, which requires additionally this last condition. This constitutes a definite advantage of CSMW over other TFD based methods, which require efficient adaptation strategies. Parallel, parametric and especially signal eigenspace or subspace base methods, offer increased frequency resolution and robustness to noise [3], especially in the case of multiple harmonic components.

According to the proposed method, first a set of wavelet transforms of the signal are obtained, using a structure of Complex Shifted Morlet Wavelets. In principle, there are no constraints on the center frequencies

and the bandwidths of the individual wavelets, as well as on the number of wavelets used, apart from the fact that the number of wavelets should be greater or equal to the number of harmonic components anticipated. In this way, a number of complex signals result in the time domain, equal to the number of Morlet wavelets selected, each one of which contains only that part of the signal frequency range allowed by the corresponding wavelet.

However, since multiple frequencies may coexist in the frequency band of a single wavelet, or equivalently, a time dependent instantaneous frequency may coexist in different wavelet bands during the time, the task of effectively separating the individual instantaneous frequencies emerges. This is possible due to the subspace rotational invariance property of the entire set of the resulting complex signals, a property quite similar the rotation invariance property of the signal itself [6]. Therefore, any appropriate variant of subspace based methods can be efficiently used for this task [5], [6], [7].

However, contrary to the classical subspace methods which are applied to the signal itself, the method proposes the application of the method after the signal has been appropriately transformed by an appropriate wavelet structure. In this way, the performance of the subspace based approach is increased, since the desired time-frequency features of the signal are enhanced, while simultaneously, the undesired frequency components, as well as the noise, are suppressed.

Equally important is the fact, that the method provides a means for calculating the number of the resulting harmonic components. A relevant indicator for that is the number of the non-zero singular values of the corresponding singular value decomposition problem, which results as a consequence of the signal subspace invariance property [6]. Moreover, since the instantaneous frequency calculations are performed on each time instant, the resulting singular values are also dependent, providing valuable information on the possibly time variable dynamic structure of the signal.

It should be noted that the concept of preprocessing a signal by an appropriate filter bank is not new, as for e.g. presented by Gabor dictionaries in matching pursuit [8], or by Gabor filters [9], [16] before the application of an instantaneous frequency and amplitude calculation procedure. Moreover certain preliminary approaches [20] have been proposed for the direct calculation of a single instantaneous amplitude and frequency of the signal from a set of two different filters. The main novelty in the current paper is the introduction of the rotational invariance approach for the processing of the results of the filter bank, as well as the general, flexible, adaptable and efficient structure of this filter bank in the form of Complex Shifted Morlet Wavelets.

The rest of the paper is organized as follows. The theoretical background of the method is presented in section 2. Applications in synthetic signals are presented in section 3. They include a sum of harmonic

components under various amplitude, frequency and noise levels, as well as amplitude and frequency modulated signals with possibly overlapped regions. Finally, applications to instantaneous frequency estimation in experimental and industrial measurements are presented in section 4.

2. Theoretical background

The complex Morlet wavelet is defined in the time domain as a harmonic wave with a frequency f_c multiplied by a Gaussian time domain window:

$$Y(t) = ce^{-\sigma^2 t^2} e^{-j2\pi f_c t} \quad (1a)$$

where c is a positive integer. The wavelet parameters are typically chosen as:

$$c = 2\sigma / \sqrt{\pi} \quad (1b)$$

$$f_c = \omega_c / 2\pi \quad (1c)$$

$$f_b = \sigma \quad (1d)$$

According to the above choice of c , the Fourier Transform of the Morlet wavelet is:

$$\hat{Y}(f) = \hat{Y}^*(f) = 2e^{-\frac{\pi^2}{\sigma^2}(f-f_c)^2} \quad (2)$$

where $\hat{Y}(f)$ is the complex conjugate of $\hat{Y}(f)$ and $\hat{Y}(f) = \hat{Y}^*(f)$, since $\hat{Y}(f)$ is real. This wavelet has the shape of a Gaussian window in the frequency domain. The center frequency of the window is defined by the frequency f_c of the harmonic component and the bandwidth of the window is determined by the parameter σ .

The scaling of the mother wavelet, simultaneously shifts the location of the window, affects the height of the window and modifies the bandwidth as well. In this way, the bandwidth of the wavelet cannot be chosen independently from the central frequency. For this reason, instead of scaling, just shifting has been proposed [21],[22].

For a specific choice of the central frequency and the bandwidth, the wavelet coefficients of a signal $x(t)$ can be obtained in the time domain through the Inverse Fourier Transform of the multiplication of the Fourier transform of the signal and the Fourier Transform of the wavelet:

$$W_{f_c, f_b}(t) = F^{-1} \left\{ X(f) \hat{Y}_{f_c, f_b}^*(f) \right\} \quad (3)$$

where $X(f)$ is the Fourier Transform of the signal $x(t)$, $F\{\}$ denotes the Fourier Transform of a function and $F^{-1}\{\}$ denotes the Inverse Fourier Transform.

For the case of a simple harmonic signal:

$$x(t) = A \cos(\omega t) \quad (4a)$$

Eq (3) leads to the following complex signal $w(t)$ under proper conditions [4]:

$$w(t) = Ag \exp(j\omega t) \quad (4b)$$

$$g = \exp\left[-\left(\frac{\omega_c - \omega}{2\sigma}\right)^2\right] \quad (4c)$$

In the case of a processing of signal $x(t)$ containing P harmonic components:

$$x(t) = \sum_{k=1}^P A_k \cos(\omega_k t + \varphi_k) \quad (5)$$

with a set of M CSMW, eq. 4 becomes:

$$w_i(t) = \sum_{k=1}^P A_k g_{ik} \exp[j(\omega_k t + \varphi_k)] \text{ for } i=1, \dots, M \quad (6a)$$

$$g_{ik} = \exp\left[-\left(\frac{\omega_{ci} - \omega_k}{2\sigma_i}\right)^2\right] \quad (6b)$$

Denoting by T the uniform sampling time, eq. (6a) can also be written at a time instant $t_n = nT$, as:

$$w_i(nT) = \sum_{k=1}^P g_{ik} s_k \quad (7a)$$

$$s_k = A_k \exp(j\varphi_k) q_k^n \quad (7b)$$

or in complex matrix form:

$$\mathbf{w}(n) = \mathbf{G} \cdot \mathbf{s} \quad (8a)$$

$$[\mathbf{w}(n)]_i = w_i(nT) \quad (8.b)$$

$$[\mathbf{G}]_{ik} = \mathbf{g}_{ik} \quad (8.c)$$

$$[s]_k = s_k \quad (8.d)$$

For the next time instant $t_{n+1} = (n+1)T$, equation (8a) becomes:

$$\mathbf{w}(n+1) = \mathbf{G} \cdot \boldsymbol{\Phi} \cdot \mathbf{s} \quad (9a)$$

$$\boldsymbol{\Phi} = \begin{bmatrix} q_1 & & 0 \\ & \ddots & \\ 0 & & q_P \end{bmatrix} \quad (9b)$$

$$q_k = \exp(j\omega_k T) \quad (9c)$$

A careful observation of equations (8) and (9) reveals that they are exactly in the form of equations (9) and (10) of the well-established ESPRIT algorithm [6]. The basic concept of this algorithm is to exploit the rotational invariance of the signal subspace, in order to determine the individual frequencies of the signal just from the diagonal values of the matrix Φ (eq 9b), independently from the rest of the values of the signal.

Towards this direction, many efficient algorithms have been established, a typical case of which is the TLS algorithm [6]. An appropriate adaptation of this algorithm to the specific case consists of the following steps:

- (1) At each time instant $t_n = nT$ form a “data matrix” \mathbf{Z} , with dimensions $2M \times N$.

$$\mathbf{Z} = \begin{bmatrix} \mathbf{w}(n-N-1) & \mathbf{w}(n-N) & \mathbf{w}(N-k-1) & \mathbf{w}(n-1) \\ \mathbf{w}(n-N) & \mathbf{w}(n-N+1) & \cdots & \mathbf{w}(n) \\ \mathbf{w}(N-k) & \cdots & \mathbf{w}(n) & \end{bmatrix} \quad (10)$$

- (2) Perform the Singular Value Decomposition of \mathbf{Z} . The SVD results to a diagonal matrix \mathbf{D} where the number of the non-zero diagonal elements of \mathbf{D} (singular values) indicates the number of the harmonic components of the signal.

$$\mathbf{Z} = \mathbf{U} \cdot \mathbf{D} \cdot \mathbf{V}^T \quad (11)$$

where $\mathbf{U} : 2M \times 2M$, $\mathbf{D} : 2M \times N$, $\mathbf{V} : N \times N$

- 3) Select the P vectors of \mathbf{U} corresponding to the P largest singular values, where:

$$\mathbf{U}_P = [\mathbf{u}_1, \mathbf{u}_2, \dots, \mathbf{u}_P] \quad (12)$$

- (4) Arrange $\underline{\mathbf{U}}$ as:

$$\mathbf{U}_P = \begin{bmatrix} \mathbf{U}_1 \\ \mathbf{U}_2 \end{bmatrix} \quad (13)$$

where $\mathbf{U}_1 : M \times P$, $\mathbf{U}_2 : M \times P$

and form the matrix Ψ :

$$\Psi = (\mathbf{U}_1^H \mathbf{U}_1)^{-1} \mathbf{U}_1^H \mathbf{U}_2 \quad (14)$$

- (5) Perform the eigendecomposition of Ψ . Based on the rotational invariance properties of Φ and Ψ , the eigenvalues of Ψ are the same as those of Φ [6]. Hence, the instantaneous frequencies ω_i can be recovered from q_i (eq. 9c).

3. Implementation on synthetic signals

3.1 Sum of two harmonic components (Test case 1)

A sum of two harmonic components is considered, similar in purpose and form to a corresponding signal used in [19]:

$$x(t)=\cos(2\pi t)+A\cos(2\pi ft) \quad (15)$$

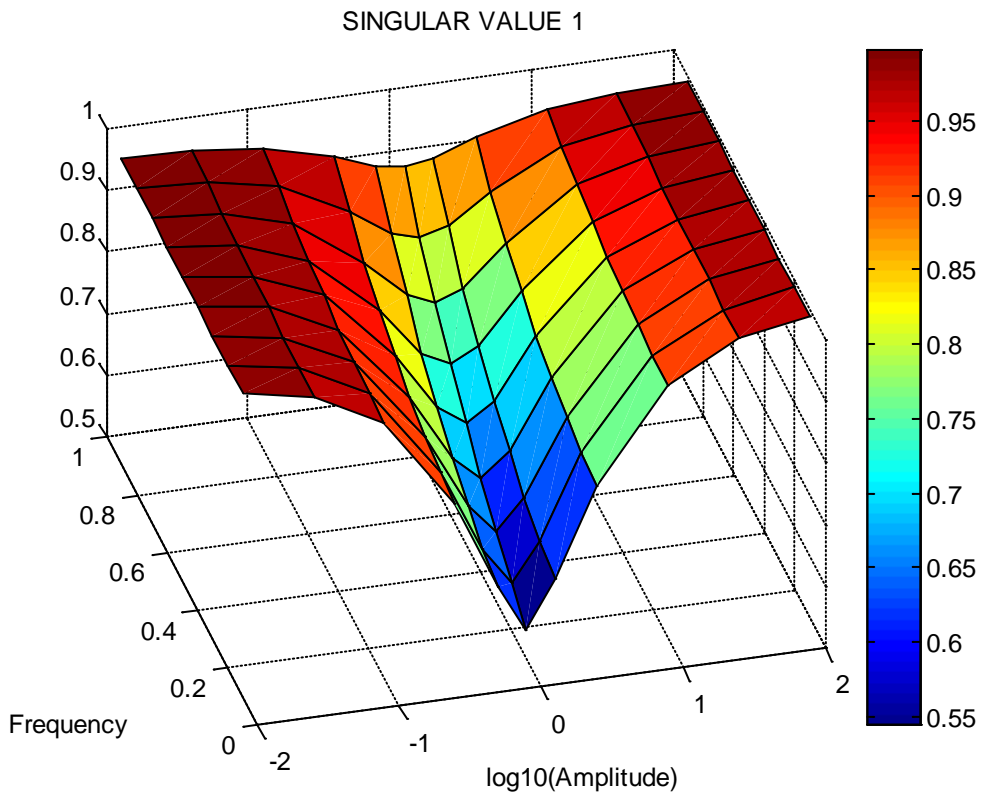
The amplitude and the frequency of the second signal, are considered to vary in the range $A=[0.01, 100.]$, $f=[0.1, 0.9]$. Also a white Gaussian noise is added with a signal to noise ratio with values: $\text{SNR} \in \{100, 50, 20, 10\}$.

A structure of $M=12$ CSMW is used, with center frequencies f_{ci} and bandwidths uniformly selected as per Table 1, while the ESPRIT algorithm is implemented for a number of $P=2$ frequencies.

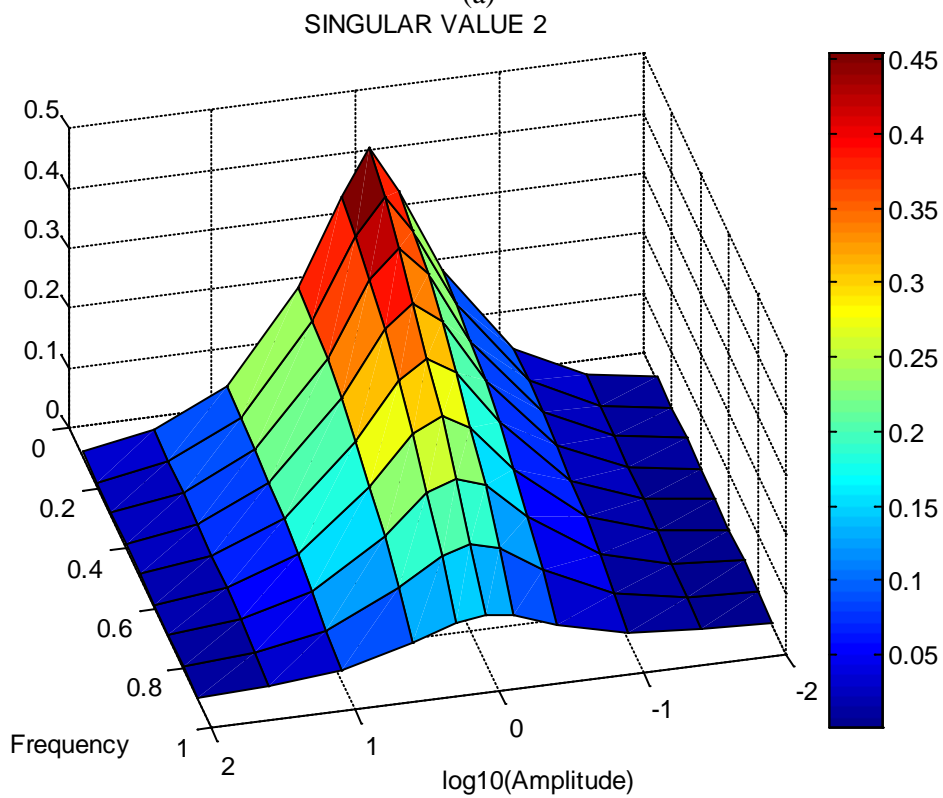
<i>Center Frequency (f_{ci})</i>	0.1	0.2	0.3	0.4	0.5	0.6	0.7	0.8	0.9	1.0	1.1	1.2
<i>Bandwidth ($\sigma_{i=f_{bi}}$)</i>	0.1	0.2	0.2	0.2	0.2	0.2	0.2	0.2	0.2	0.2	0.2	0.2

Table 1. Center Frequencies and bandwidths of the CSMW structure used in section 3.1

The first two singular values for a sum of harmonic components under various amplitudes and frequencies are depicted in Fig. 1 for a $\text{SNR}= 100$. As it can be observed, contrary to other frequency estimation approaches [19], [20], a second harmonic component is clearly foreseen only in the case where the two signals have amplitudes and frequencies well separated.



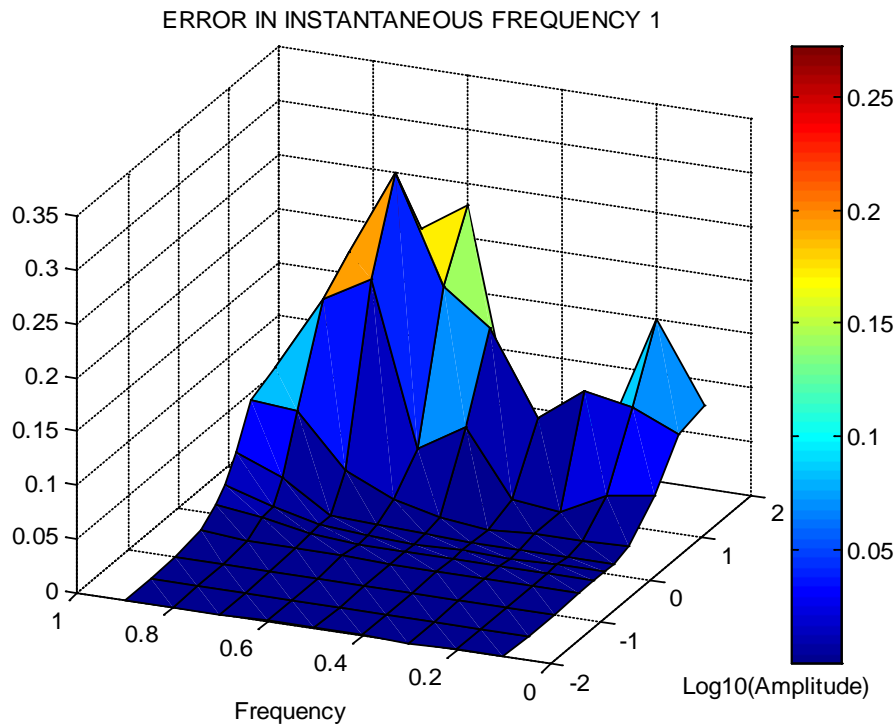
(a)



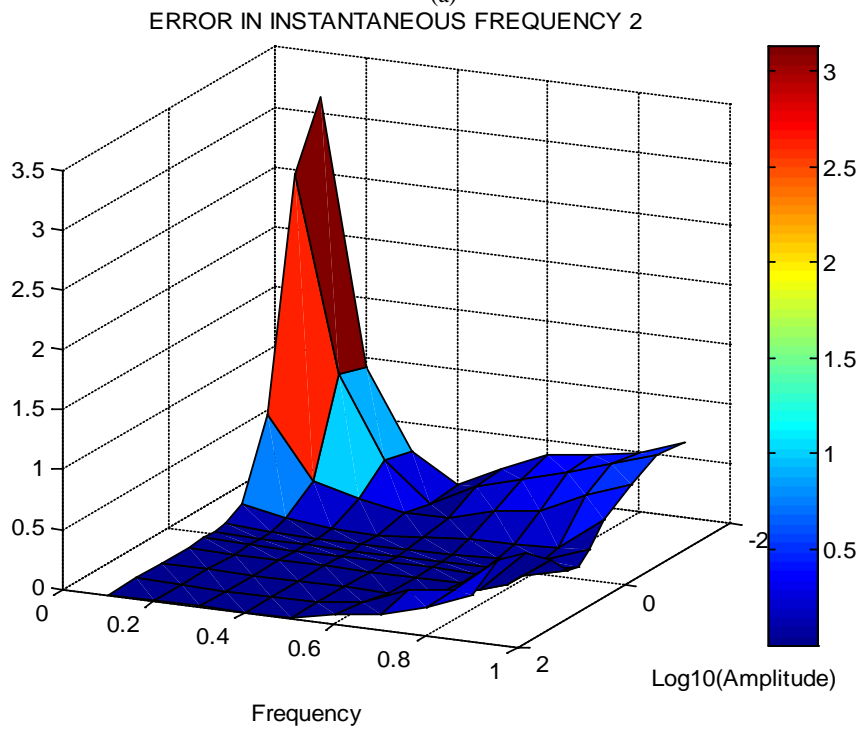
(b)

Figure 1: First two singular values (a & b) of a sum of harmonic components for various amplitudes A and frequencies f of the second harmonic component and for a SNR= 100.

The errors in the estimation of the two frequencies are presented in Fig. 2 for a significant noise level of SNR=10. The errors remain insignificant, with the exception of the cases where the amplitude of the corresponding signal is practically negligible with respect to that of the corresponding dominant signal. Also, the errors are practically nil in the case of SNR=100.



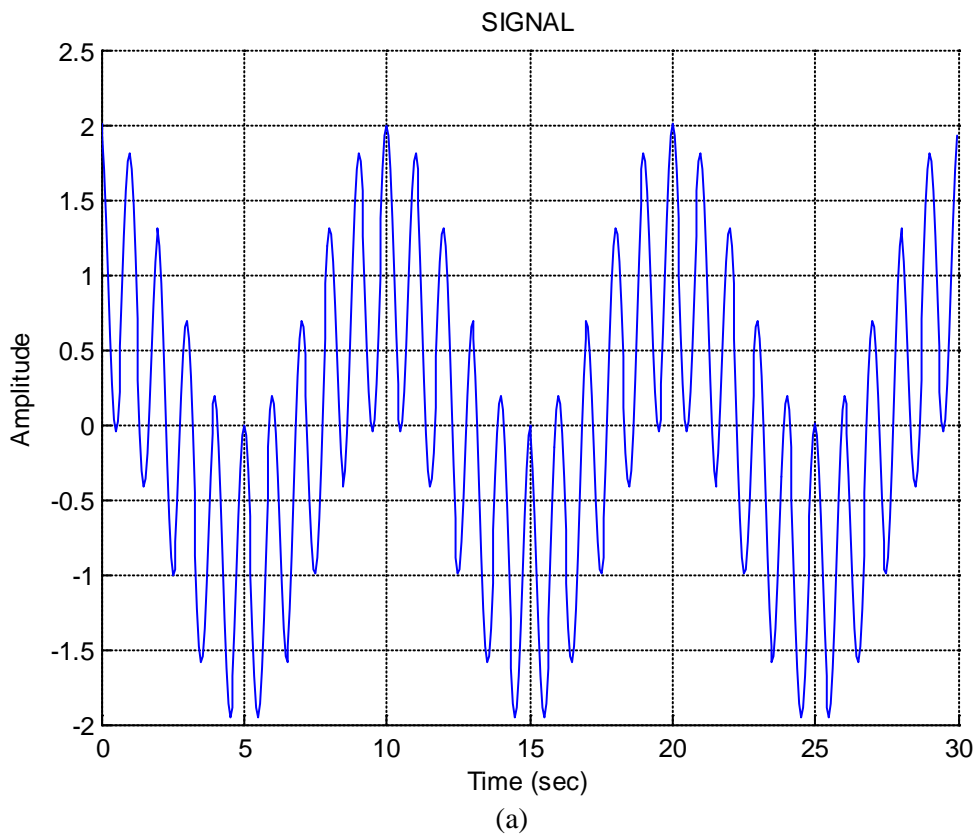
(a)



(b)

Figure 2: Errors in the estimation of the frequencies of the two harmonic components (a &b) for various amplitudes A and frequencies f of the second harmonic component and for SNR= 10.

Several cases of signal waveforms are presented in Figs 3 to 5. As it can be verified by those figures, a second harmonic component is clearly visible and can be practically considered as present, only when it's corresponding amplitude and frequency is well separated from the dominant one, as presented by the singular values in Fig.1. Moreover, in the cases of a significant noise level of SNR=10, despite the significant distortion of the signal, the dominant frequency is accurately predicted. Also, the large frequency estimation errors in the case of noise depicted in Fig. 2 can be easily justified, since the second component is practically negligible compared to the noise level. It should be mentioned that the results presented in [18],[19] do not take into account the noise effects.



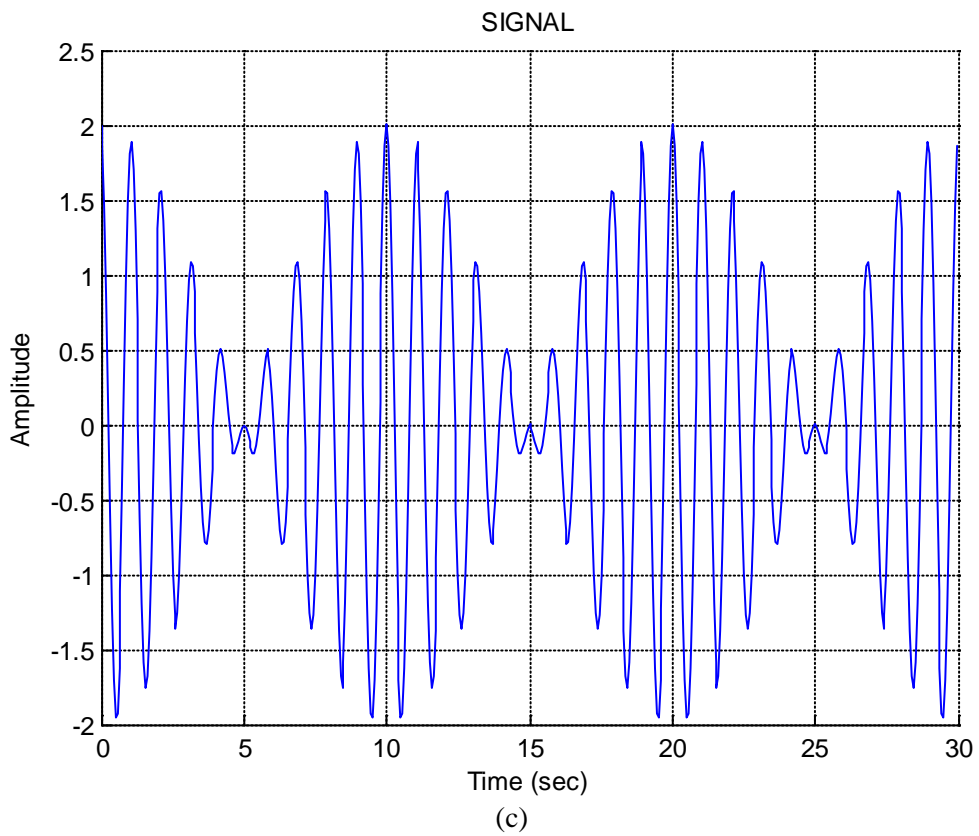
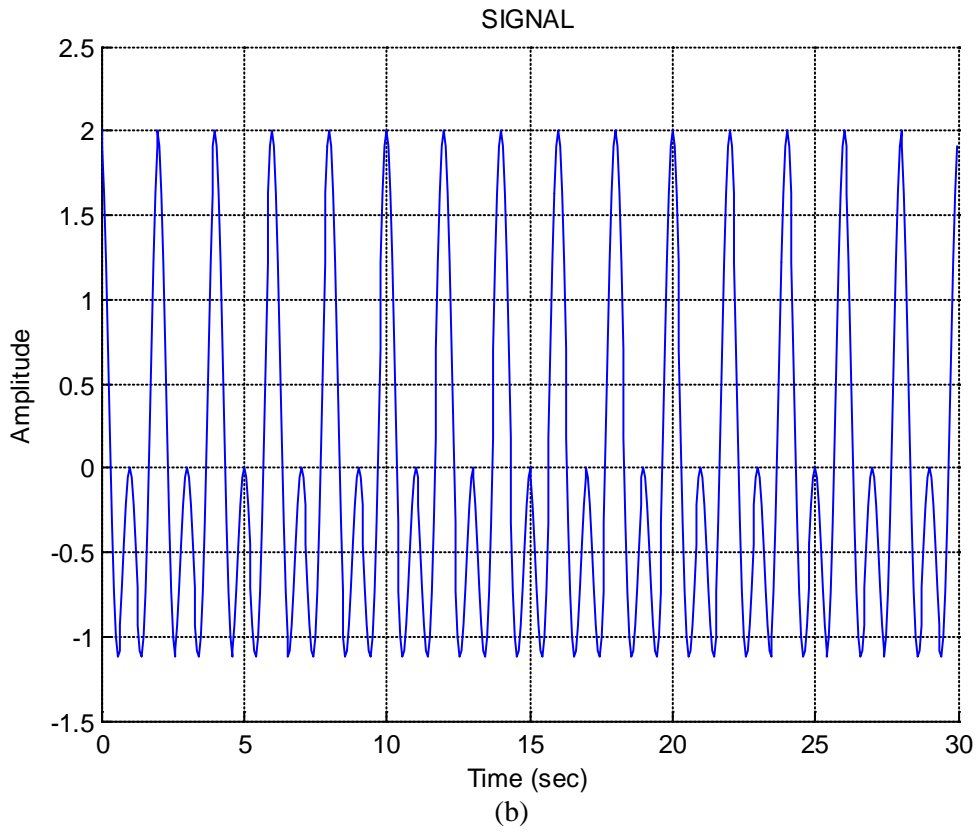


Figure 3: Signal waveforms with signal harmonic components of equal amplitude ($A=1$). (a) $f=0.1$, (b) $f=0.5$, (c) $f=0.9$, $SNR=100$.

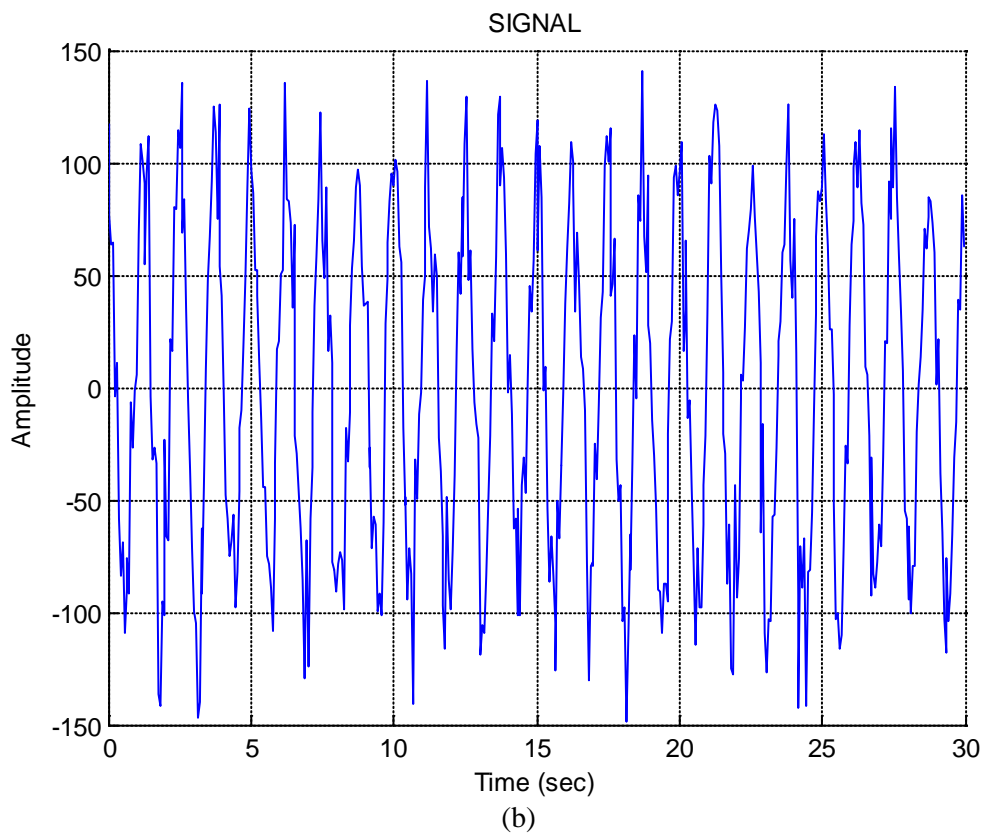
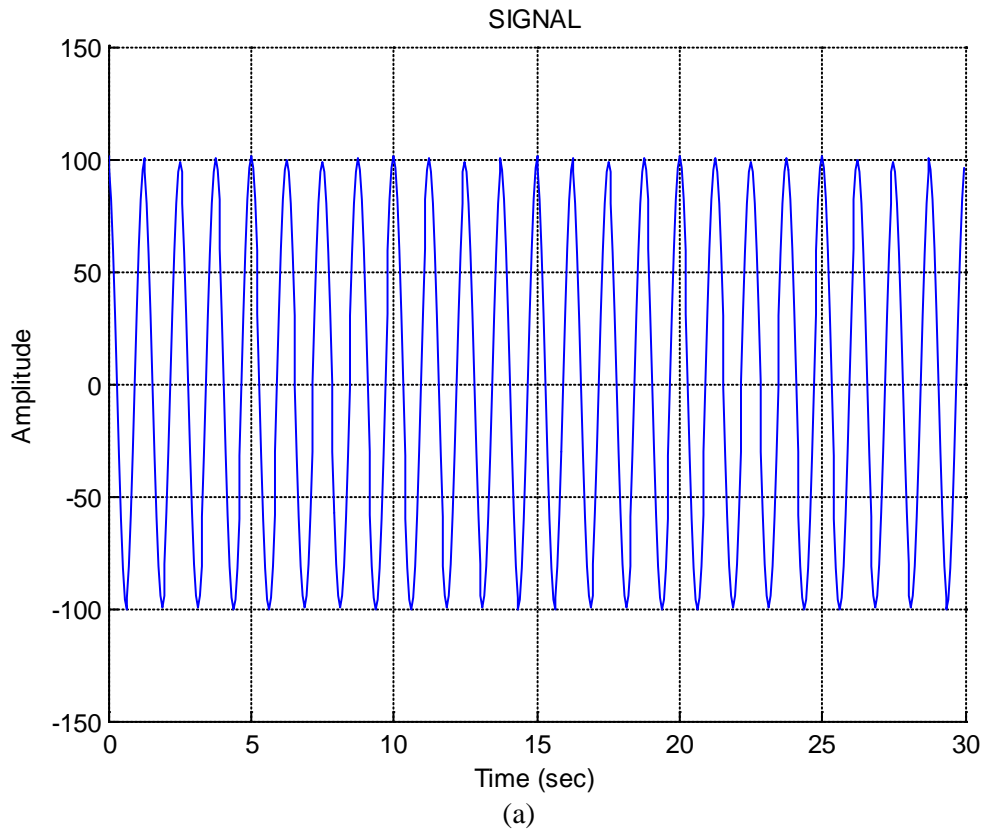


Figure 4: Signal waveforms with a second signal harmonic component of $A=100$ and $f=0.8$ (a) SNR=100, (b) SNR=10.

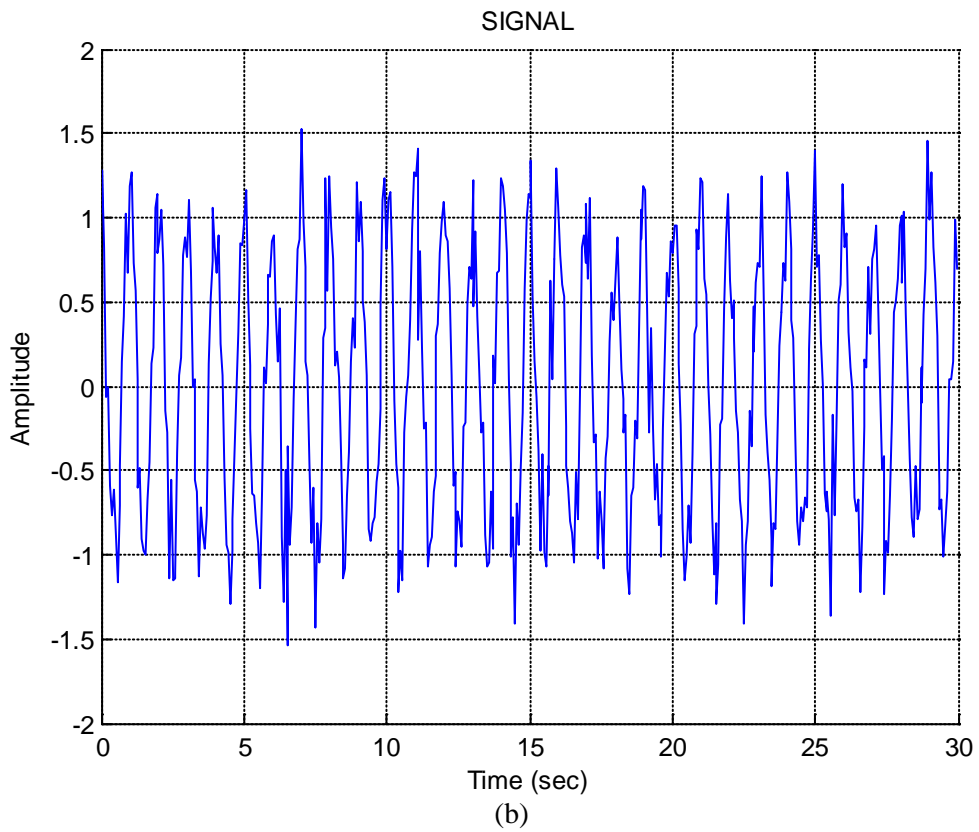
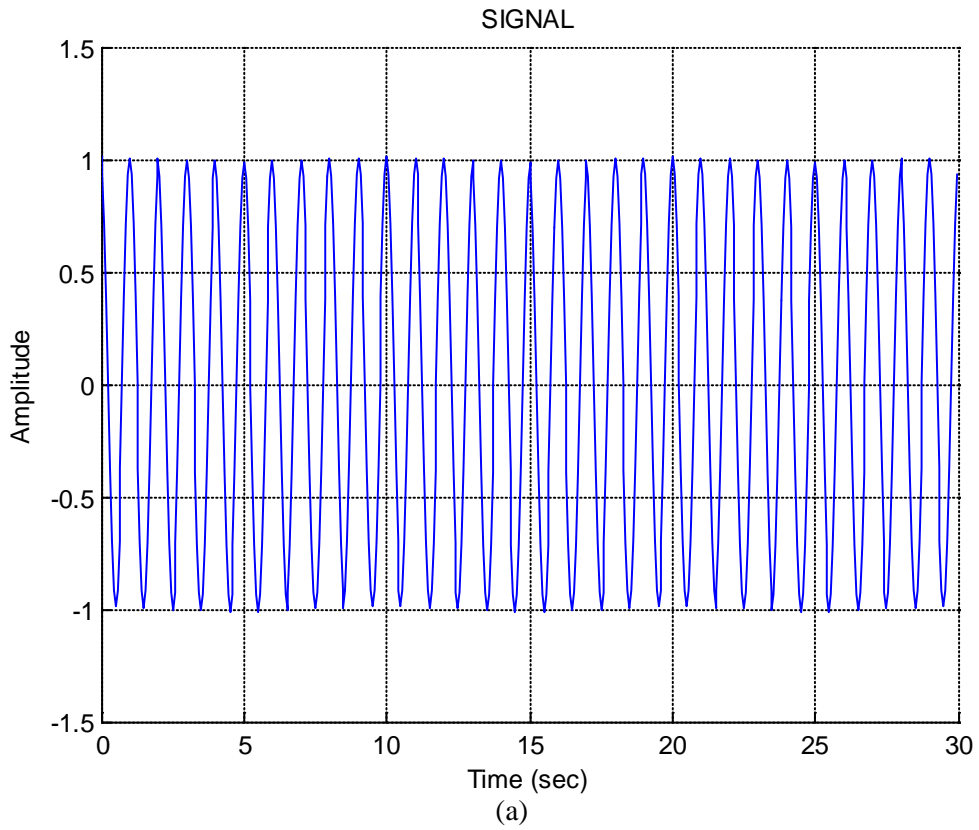


Figure 5: Signal waveforms with a second signal harmonic component of $A=0.01$ and $f=0.1$ (a) SNR=100, (b) SNR=10.

3.2 Amplitude modulated signals (Test case 2)

The two component Amplitude Modulated signal, defined in Eqs (41) and (42) of [15] is analyzed. Initially, the signal is tested with exactly the following data [15]:

$$x(t) = A_1(t)\sin(2\pi f_1 t) + A_2(t)\sin(2\pi f_2 t) \quad (16a)$$

$$A_1(t) = 1 + 0.5 \cos(2\pi f_{01} t) \quad (16b)$$

$$A_2(t) = 0.2 \quad (16c)$$

where $f_1=500\text{Hz}$, $f_2=550\text{Hz}$, $f_{01}=10\text{Hz}$. The waveform of the signal is depicted in Fig.6.

The signal is initially analyzed with a structure of $M = 7$ CSMW, with center frequencies f_{ci} and bandwidths uniformly selected as per Table 2, while the ESPRIT algorithm is implemented for a number of $P=2$ frequencies.

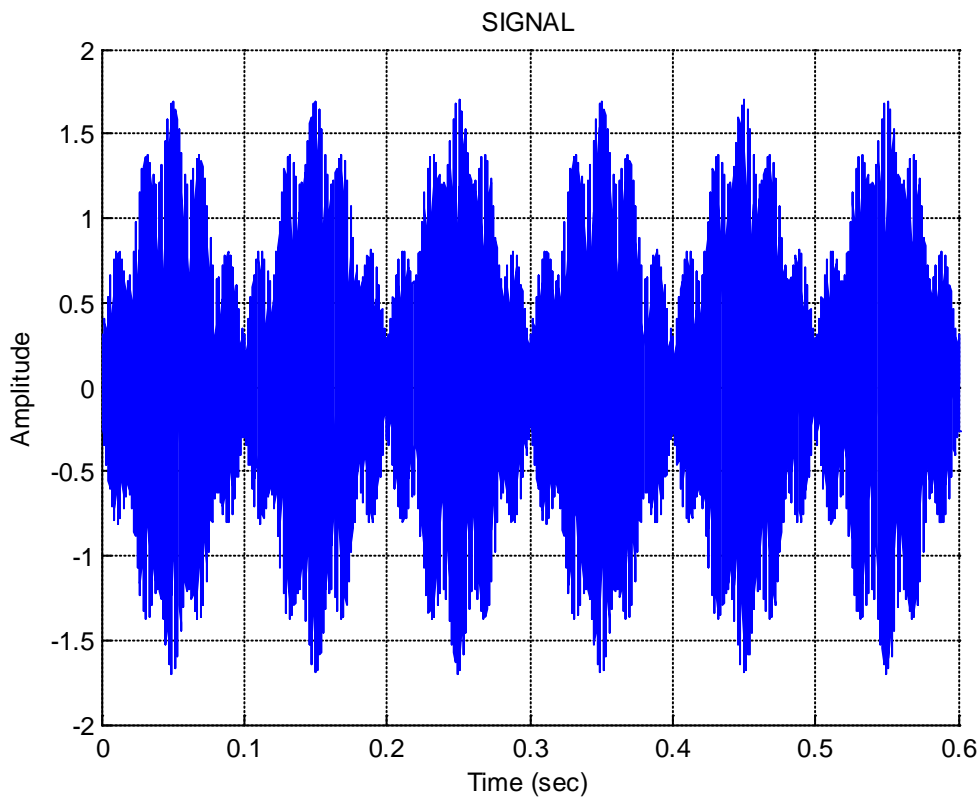


Figure 6: Two component Amplitude Modulated signal used in section 3.2 (Test case 2).

<i>Center Frequency (f_{ci})</i>	490	500	510	520	530	540	550
<i>Bandwidth ($\sigma_i = f_{bi}$)</i>	100	100	100	100	100	100	100

Table 2. Center Frequencies and bandwidths (Hz) of the initial CSMW structure used in section 3.2

The spectrum of the signal of Fig. 6, together with the initial CSMW structure of Table 2 is presented in Fig. 7, the resulting singular values are presented in Fig. 8, and the resulting instantaneous frequencies are

presented with blue lines in Fig. 9. These values of the instantaneous frequencies present to a certain extent the characteristic oscillations, inherent in the cases of overlapping frequency bands. As explained in the introduction, the real nature of this phenomenon can be only understood by a careful analysis of the analytical form of the instantaneous frequencies of signals including multiple harmonic components, as for e.g. those presented in Appendix A of [16], or more analytically in [17].

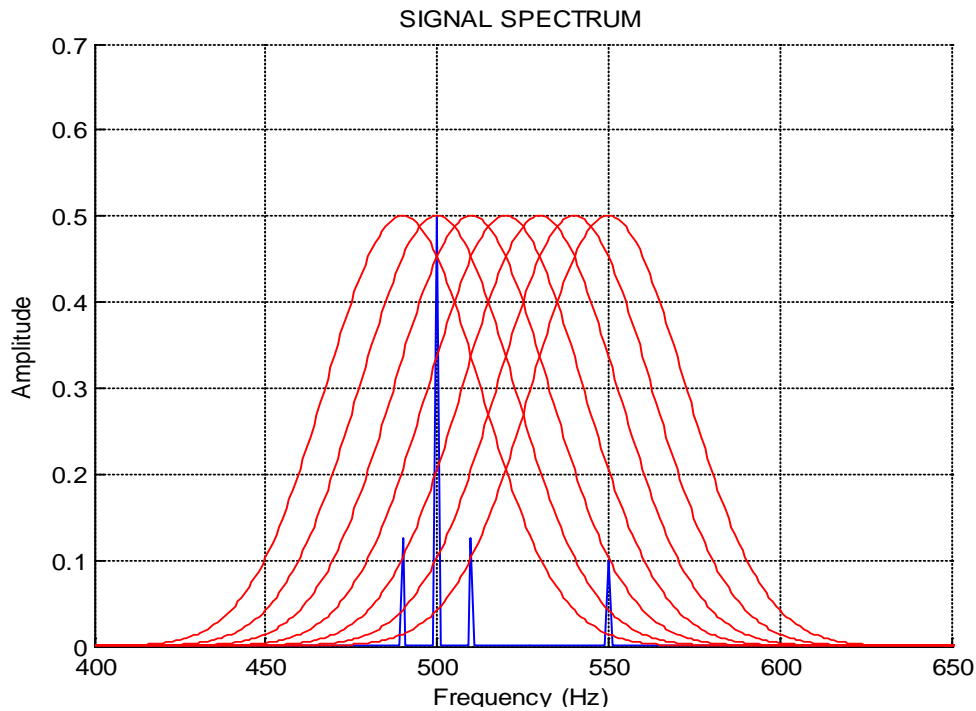


Figure 7: Spectrum of the signal of Fig. 6, together with the initial CSMW structure used in section 3.2 (Test case 2).

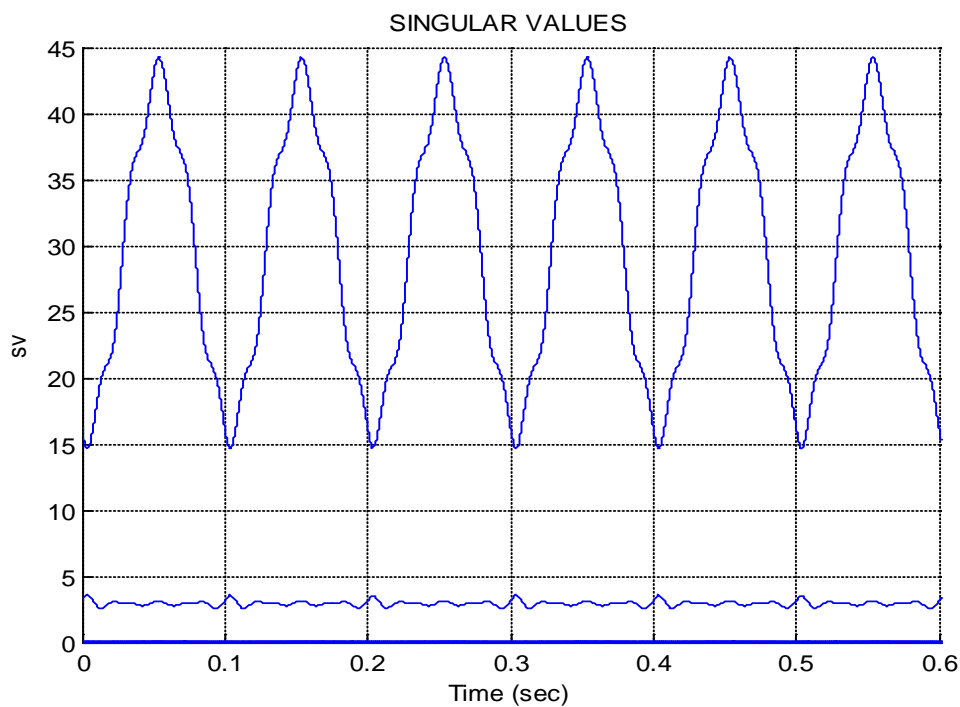


Figure 8: Singular values for the two components Amplitude Modulated signal used in section 3.2 (Test case 2).

Although a number of methods exist to mitigate this effect, in the current example, a revised CSMW was selected with $M=2$, based on the mean and the variance of the initial estimates of the instantaneous frequencies, with parameters presented in Table 3 and corresponding results presented with red lines in Fig. 9. The drastic improvement of the results indicate the significance and the potential offered by the design of an efficient CSMW structure.

<i>Center Frequency (f_{ci})</i>	500	550
<i>Bandwidth ($\sigma_i = f_{bi}$)</i>	20	5

Table 3. Center Frequencies and bandwidths (Hz) of the revised CSMW structure used in section 3.2

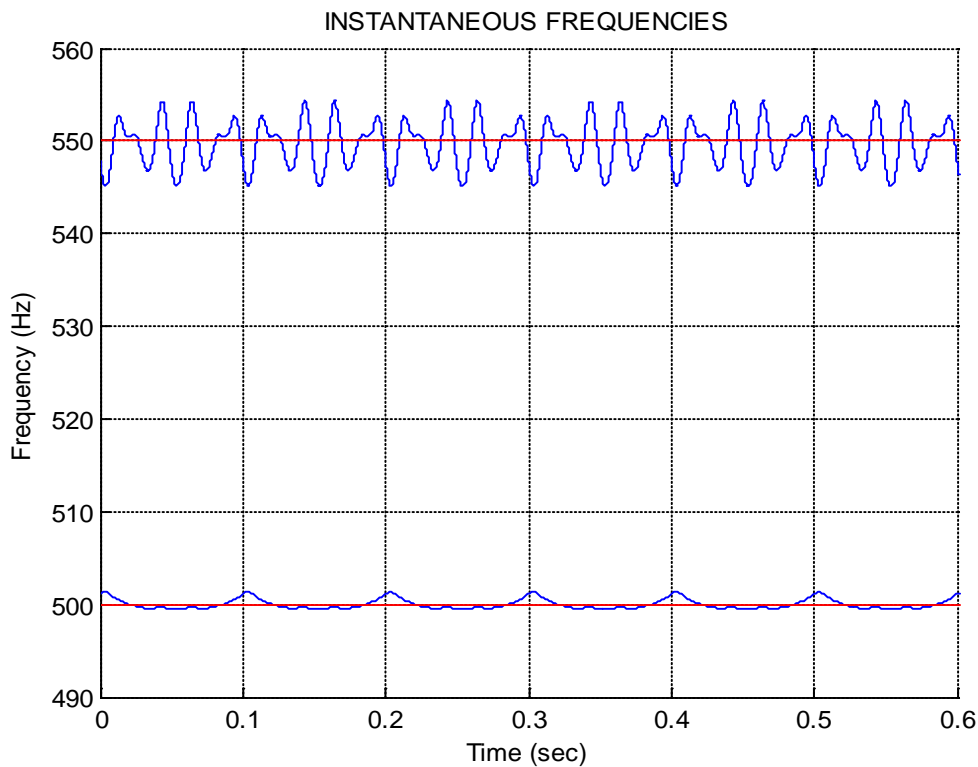


Figure 9. Instantaneous frequencies for the two component Amplitude Modulated signal used in section 3.2 (Test case 2). Blue values indicate the initial estimates of the instantaneous frequencies (CSMW structure of Table 2). Red values indicate the revised estimates of instantaneous frequencies (CSMW structure of Table 3).

Parallel, the signal was band pass filtered using as filter center frequency and bandwidth the same parameters of Table 3 and the amplitude of each signal component was calculated, using a typical order tracking algorithm [23], [24]. The resulting amplitudes are depicted in Fig. 10.

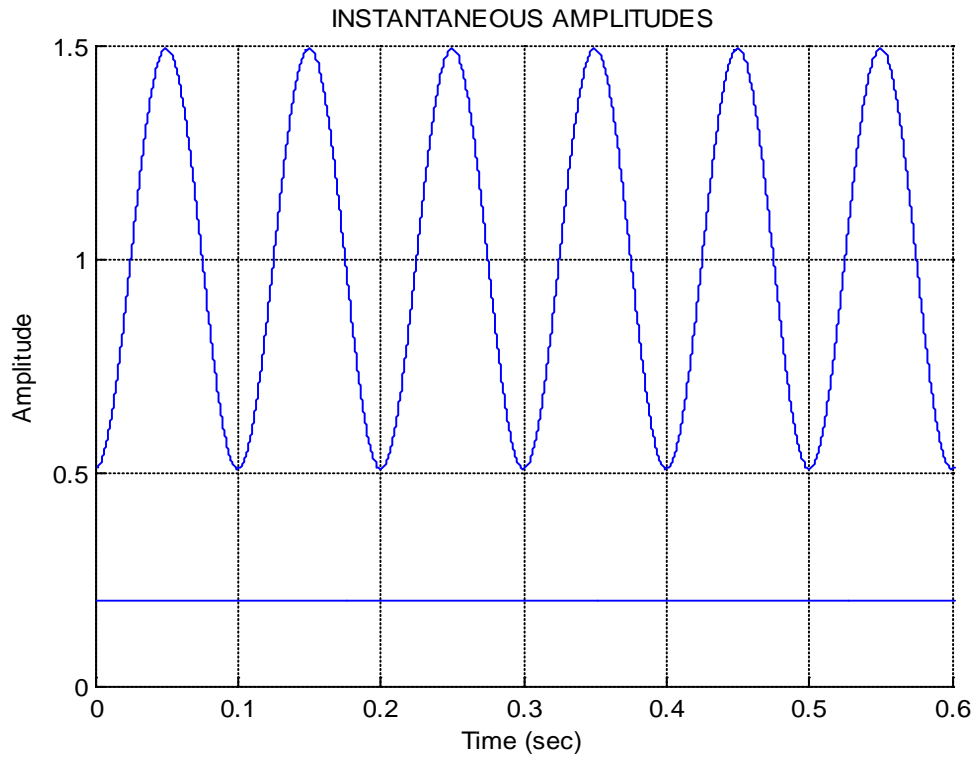


Figure 10. Instantaneous amplitudes for the two component Amplitude Modulated signal used in section 3.2 (Test case 2).

Next, the effect of the variation of the amplitude A_2 and the sensitivity to noise were calculated, according to the procedure defined in [15]. Four error measures were calculated, following Eq (46) of [15]. Two error measures SNRA1 and SNRA2 refer to the instantaneous amplitudes A_1 , A_2 and two error measures SNRF1 and SNRF2 refer to the instantaneous frequencies f_1 , f_2 .

The results are presented in Tables 4 and 5, confirming the effectiveness of the proposed method.

A_2	$SNRA1$	$SNRA2$	$SNRF1$	$SNRF2$
0.1	44.5494	31.1831	72.4110	210.4500
0.2	44.5492	55.4189	70.3753	210.4389
0.5	44.5490	88.2927	68.8877	210.4277
1	44.5489	112.2824	68.4059	210.4277
2	44.5488	121.5814	68.1709	210.4277
5	44.5488	127.7877	68.0322	210.4277
10	44.5488	130.7119	67.9863	210.4277
20	44.5488	132.0921	67.9634	210.4277

50	44.5487	132.7122	67.9497	210.4277
100	44.5484	132.8606	67.9452	210.4277
200	44.5469	132.9217	67.9429	210.4277
500	44.5367	132.9540	67.9415	210.4277

Table 4. Error measures for the amplitude modulated signals (Test case 2). Signals without noise.

A_2	$SNRA1$	$SNRA2$	$SNRF1$	$SNRF2$
0.1	43.9560	30.2164	66.6714	56.1961
0.2	43.4972	44.8719	61.5984	67.4531
0.5	40.9986	41.5756	50.7176	68.2775
1	35.7271	40.9757	45.6573	71.5610
2	30.1130	42.7722	42.1847	65.6374
5	24.8335	43.0286	34.0937	66.2983
10	17.5623	41.8423	28.8344	69.5205
20	8.9126	44.5505	18.4501	9.7370
50	3.3826	43.1342	-6.2449	65.1117
100	-0.4180	45.4183	-6.6317	63.7770
200	-7.3747	41.3686	-3.9635	66.9547
500	-14.9854	44.1604	-3.4840	70.4249

Table 5. Error measures for the amplitude modulated signals (Test case 2). Signals with SNR=10, as per [15].

3.3 Frequency modulated signals (Test case 3)

Following the test case presented in Eqs (43) to (45) of [15], two crossing chirp signals were accordingly selected with amplitudes $A_1=1$, $A_2=8$. Their corresponding frequencies f_1 , f_2 were considered also to linearly vary from 1000 Hz to 500Hz and from 500Hz to 1000Hz. The difference with [15] is that the two frequencies were allowed to coincide to a value of 750Hz for a certain time interval in the middle of the duration of the signal.

Two alternative CSMW structures were used, with corresponding data presented in Tables 6 and 7.

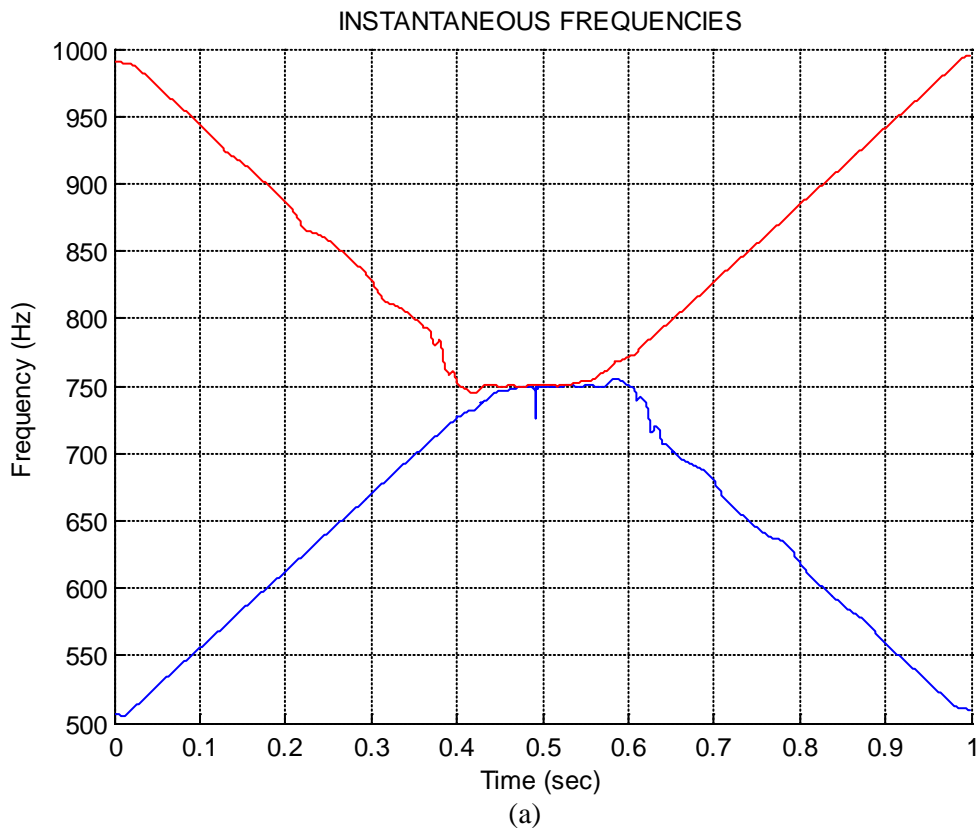
<i>Center Frequency f_{ci}</i>	500	550	600	650	700	750	800	850	900	950	1000
<i>Bandwidth ($\sigma_i = f_{bi}$)</i>	100	100	100	100	100	100	100	100	100	100	100

Table 6. Center Frequencies and bandwidths of the CSMW structure used in section 3.3 (Option A)

<i>Center Frequency f_{ci}</i>	500	600	700	800	900	1000
<i>Bandwidth ($\sigma_i = f_{bi}$)</i>	200	200	200	200	200	200

Table 7. Center Frequencies and bandwidths of the CSMW structure used in section 3.3 (Option B)

The resulting instantaneous frequencies and singular values are presented in Figs 11 and 12 for the two alternative CSMW structures. In both cases, the singular values are able to depict accurately the time variable structure of the signal. In the middle of the duration of the signal, all but the first singular value become zero, indicating that just a single harmonic component exists in the signal. Such a result is to be expected, since both instantaneous frequencies completely coincide for this interval. The instantaneous frequencies are also accurately estimated in both cases. The exception presented in Fig. 12 in the form of an oscillating behavior is to be expected, since a number of $P=2$ frequencies are requested, while just a single frequency actually is present in the signal for this interval. Such a condition generates a numerical instability.



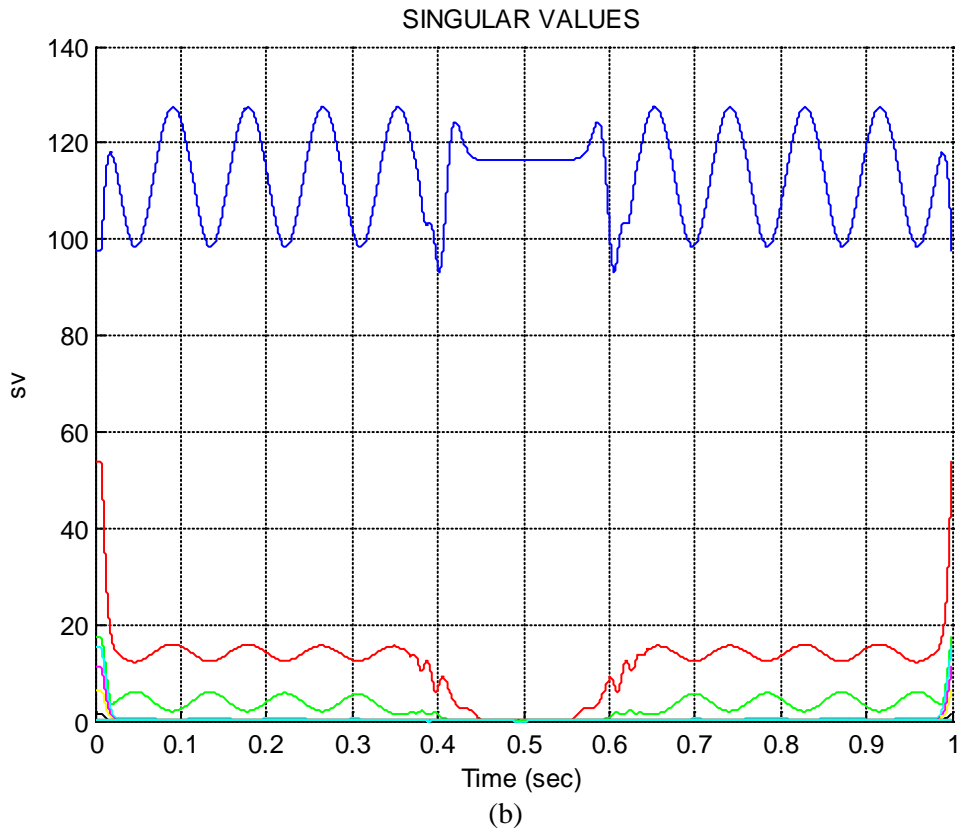
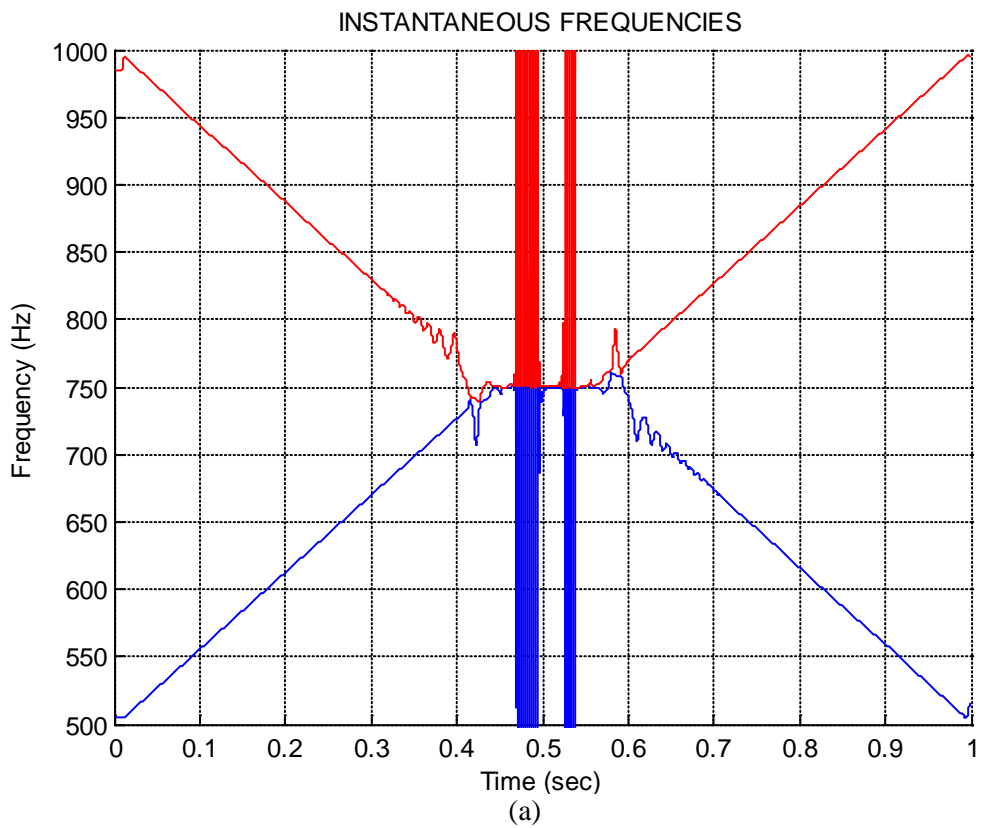


Figure 11. Instantaneous frequencies and singular values for the two component Frequency Modulated signal, using option A CSMW structure (Section 3.3, Test case 3).



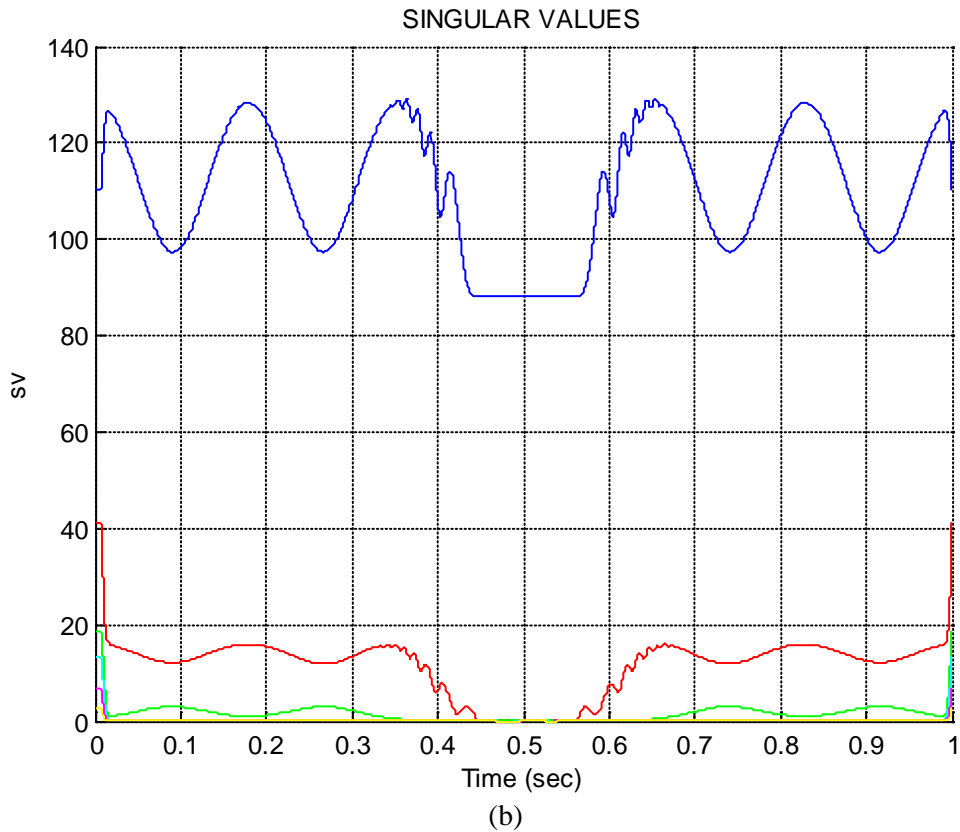


Figure 12. Instantaneous frequencies and singular values for the two component Frequency Modulated signal, using option B CSMW structure (section 3.3, Test case 3).

4. Implementation on experimental and industrial signals

4.1 Experimental test rig (Test case 4)

A vibration signal was collected at a test rig (Fig. 13) during a start-up procedure. The test rig consists of an electric motor, a shaft, a coupler for the connection between the shaft and the motor, and two bearings for the shaft seating. The rotating speed was linearly increased from 1025 rpm (17.1 Hz) to 1200 rpm (20 Hz) for a duration of 5sec. An original sampling frequency of $f_s=20\text{KHz}$ was used, while the signal was subsequently resampled to 2KHz. The parameters of the CSMW structure used are presented in Table 8.



Figure 13. Test rig for the motor startup signal used in section 4.1 (Test case 4).

<i>Center Frequency f_{ci}</i>	18	23	28	33	38	43	48	53	58	63
<i>Bandwidth ($\sigma_{i=f_{bi}}$)</i>	5	5	5	5	5	5	5	5	5	5

Table 8. Center Frequencies and bandwidths of the CSMW structure used in section 4.1

The measured vibration signal is depicted in Fig. 14 and its spectrum, together with the CSMW structure used, is presented in Fig.15. The ESPRIT algorithm was implemented for a number of $P=3$ harmonic components. The resulting singular values, as presented in Fig. 16, confirm that a number of $P=3$ harmonic components are actually present in the signal.

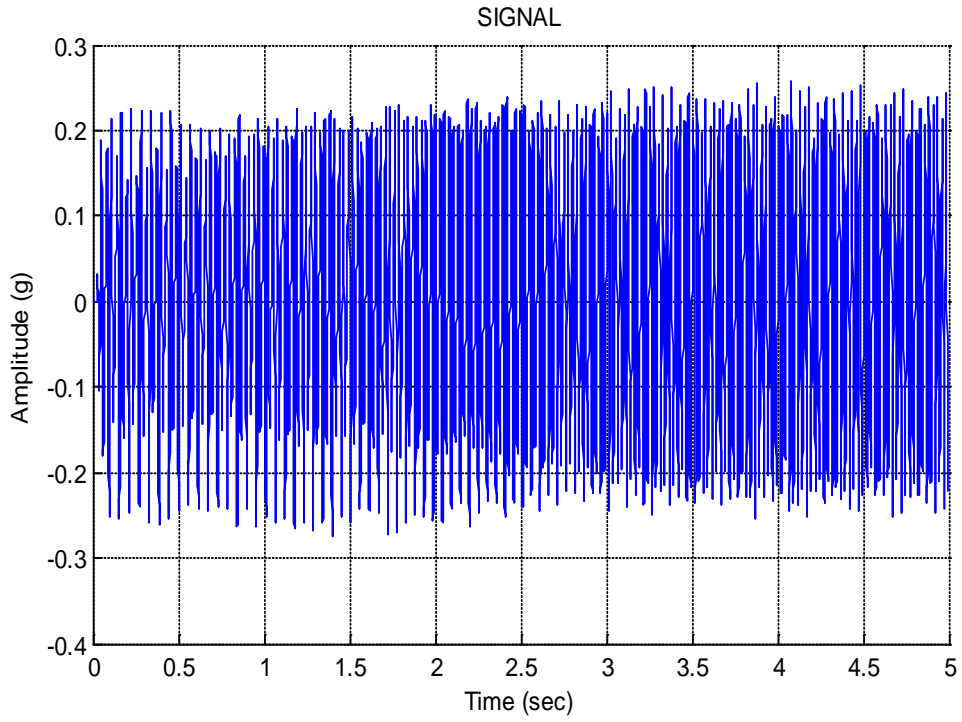


Figure 14: Vibration signal during motor startup, used in section 4.1 (Test case 4).

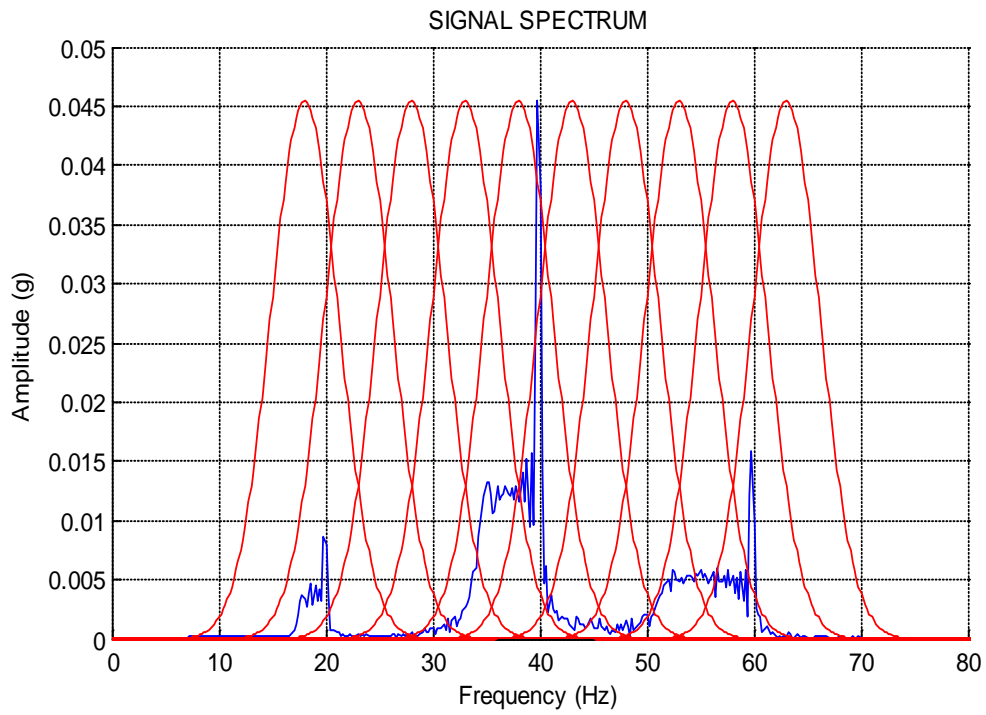


Figure 15: Spectrum of the signal of Fig. 14, together with the CSMW structure used in section 4.1 (Test case 4).

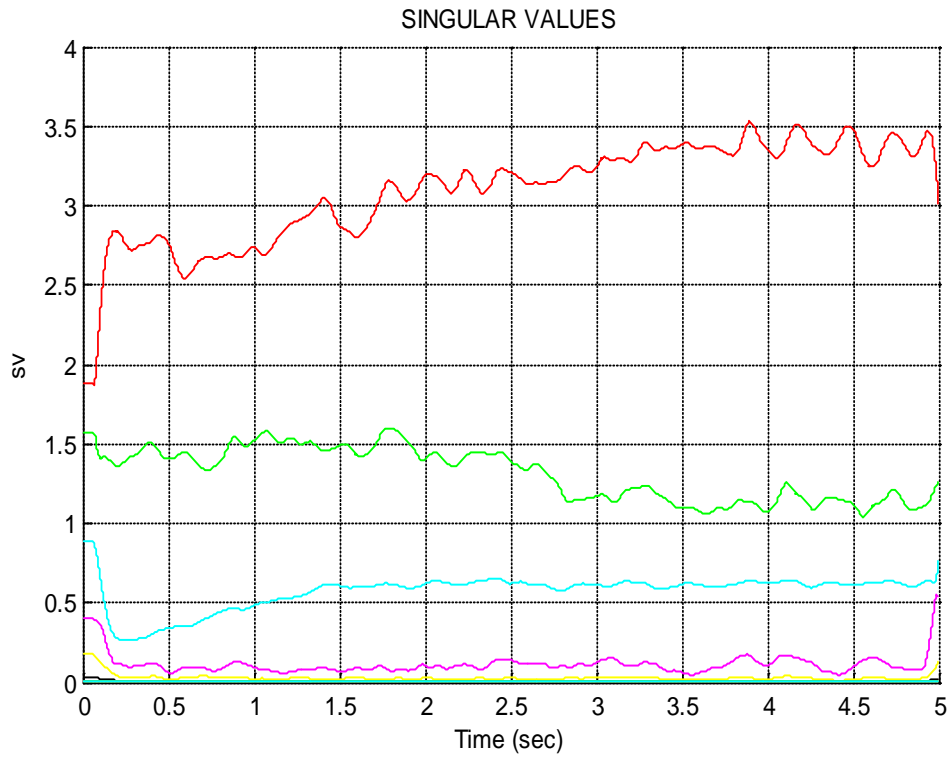
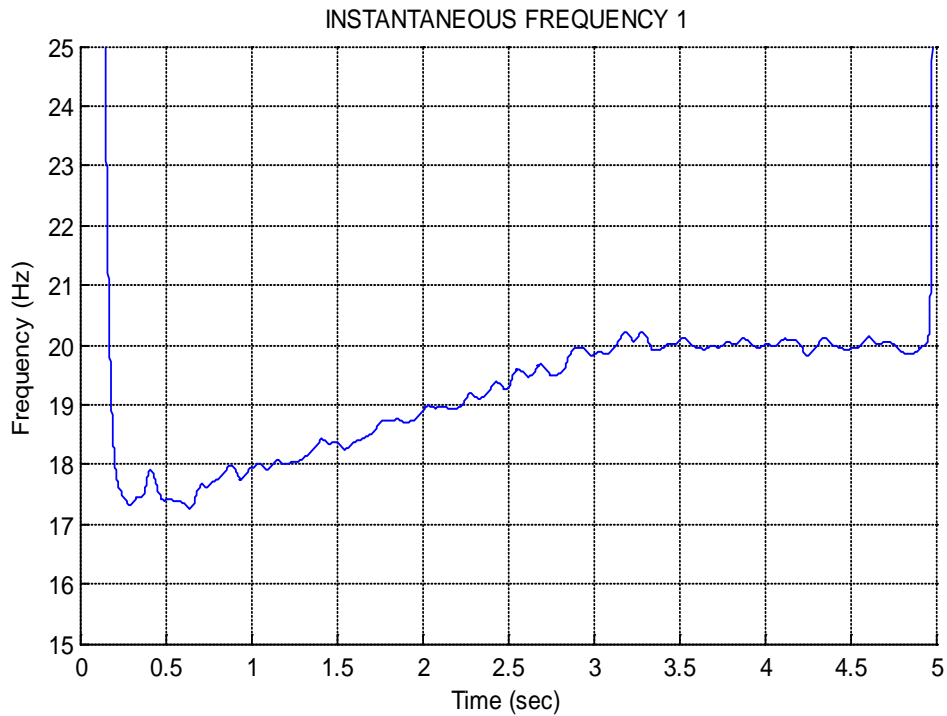
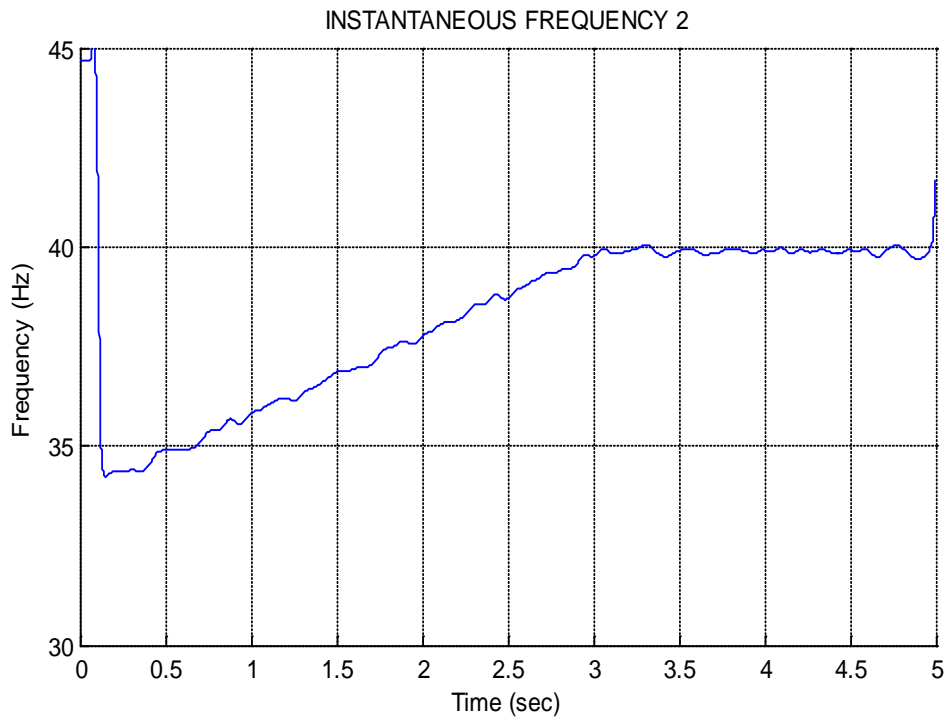


Figure 16: Singular values of the signal used in section 4.1 (Test case 4).

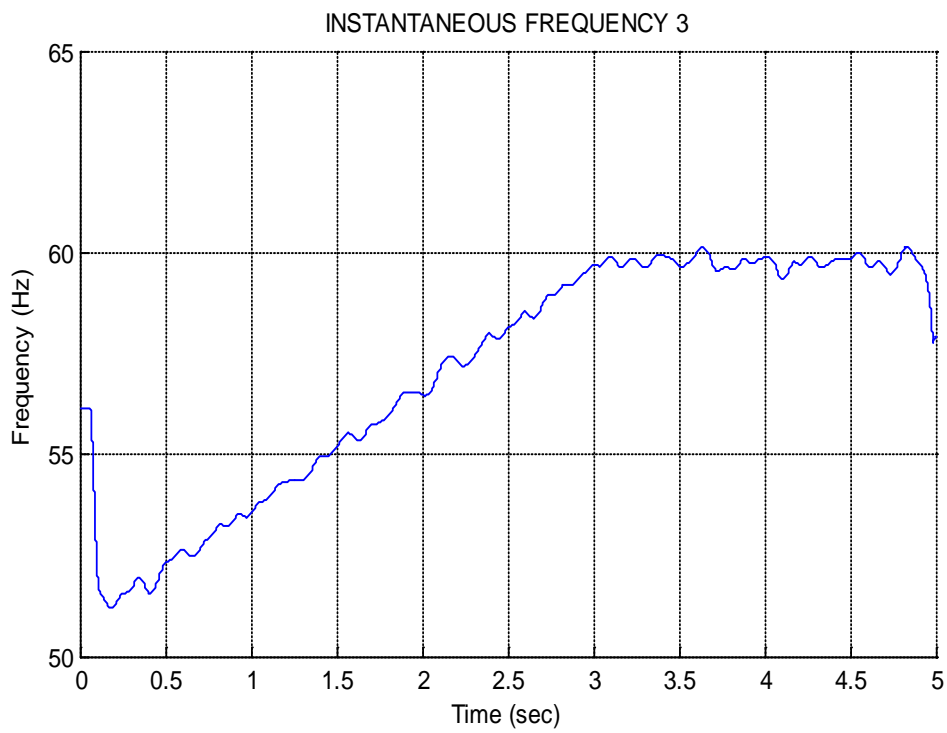
The resulting instantaneous frequencies are presented in Fig. 17 and the ratio of the higher two frequencies to the first one (harmonic orders) are presented in Fig 18, confirming the accuracy of the estimation.



(a)



(b)



(c)

Figure 17. Instantaneous frequencies (a, b & c harmonics) for the motor startup signal used in section 4.1 (Test case 4).

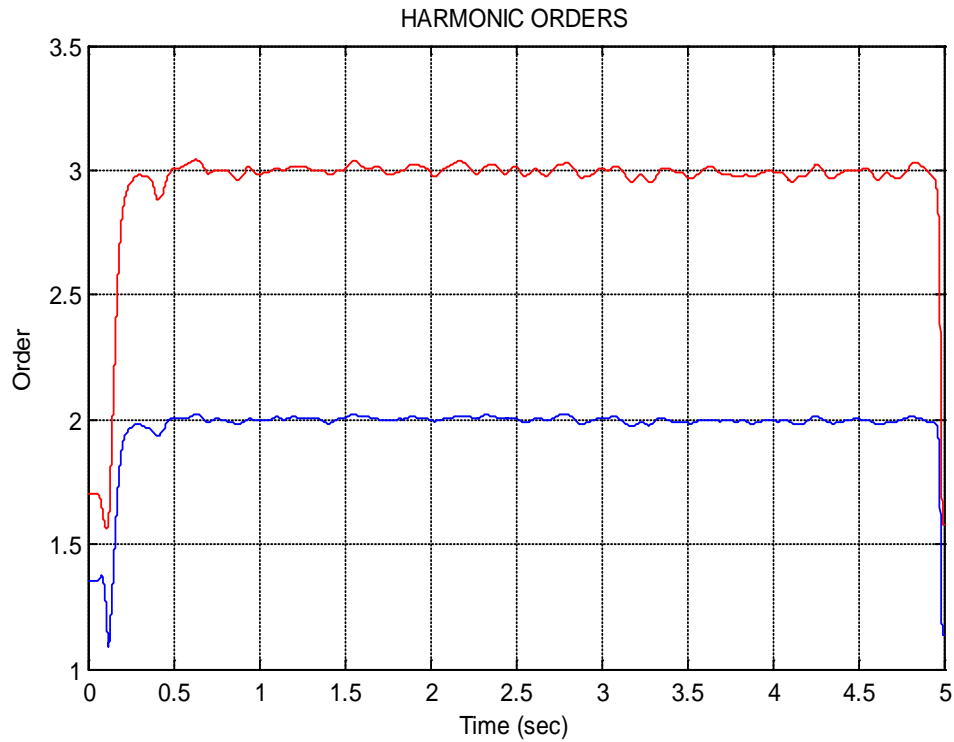


Figure 18. Ratio of second to first and third to first instantaneous frequencies (Harmonic orders) for the motor startup signal used in section 4.1 (Test case 4).

4.2 6-high rolling mill slow down

A vibration signal was collected at a 6-High rolling mill stand. The rotating speed of the working mill is in the range of 16 Hz. An original sampling frequency of $f_s=4\text{KHz}$ was used, while the signal was subsequently resampled to 1000Hz. The measured vibration signal is depicted in Fig. 19 and its spectrum, together with the CSMW structure used, is presented in Fig.20. As it can be observed, the signal contains a significant level of broadband background noise. In order to avoid the effects of this background noise, the CSMW structure was selected localized around the major peaks of the spectrum. The parameters of the CSMW structure used are presented in Table 9.

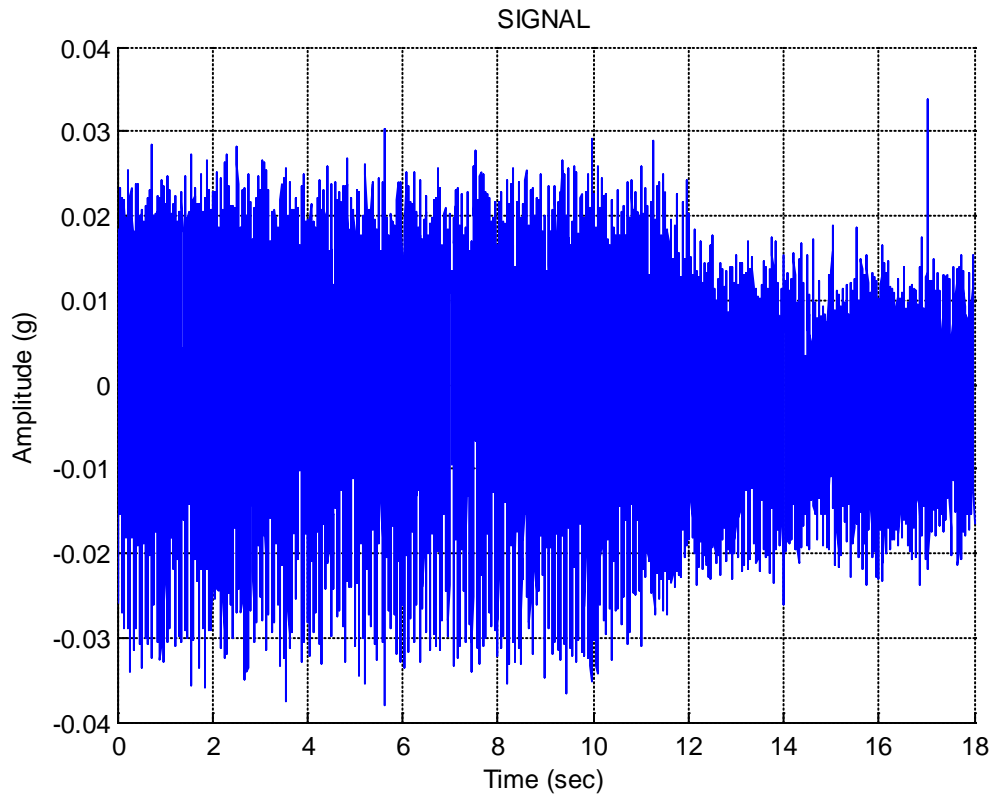


Figure 19. Vibration signal during a 6-High 6-high rolling mill slow down, used in section 4.2 (Test case 5).

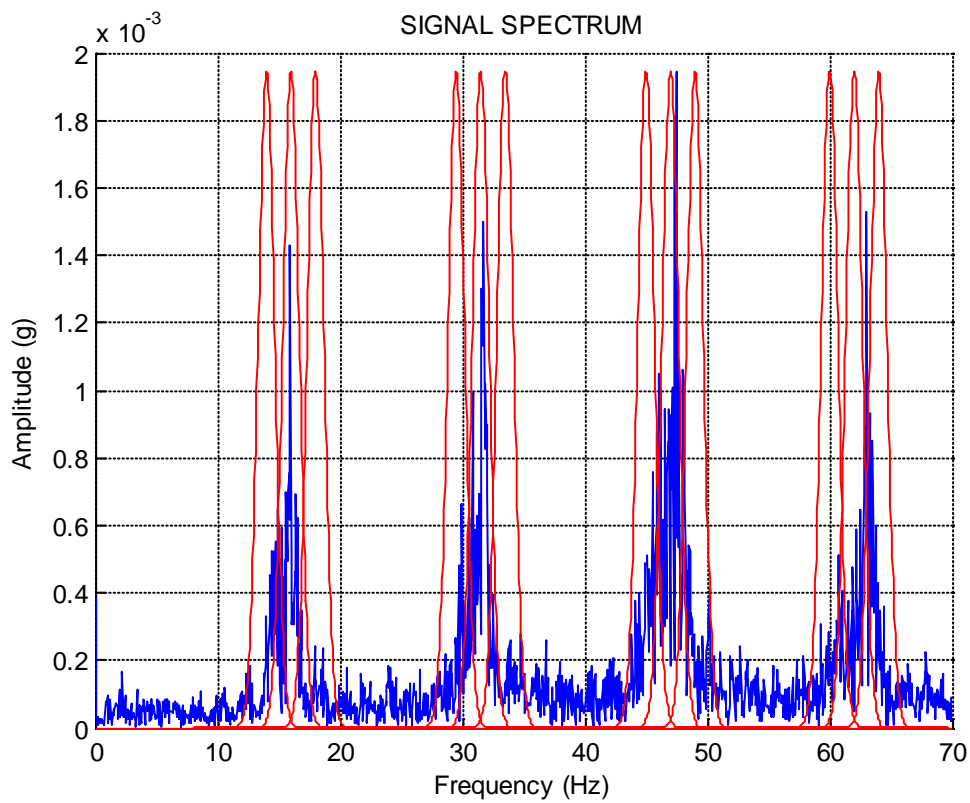


Figure 20. Spectrum of the signal of Fig. 18, together with the CSMW structure used in section 4.2 (Test case 5).

<i>Center Frequency (f_{ci})</i>	<i>Bandwidth ($\sigma_{i= f_{bi}}$)</i>
14.0	3
16.0	3
18.0	3
29.5	3
31.5	3
33.5	3
45.0	3
47.0	3
49.0	3
60.0	3
62.0	3
64.0	3

Table 9. Center Frequencies and bandwidths of the CSMW structure used in section 4.2

The ESPRIT algorithm was implemented for a number of $P=4$ harmonic components. The resulting singular values, as presented in Fig. 21, confirm that a number of $P=4$ harmonic components are actually present in the signal, through the entire analysis signal.

The resulting instantaneous frequencies are presented in Fig. 22 and the ratio of the higher three frequencies to the first one (harmonic orders) are presented in Fig. 23, confirming the accuracy of the estimation. A Kay estimator [2] was used to smooth the values of the instantaneous frequencies.

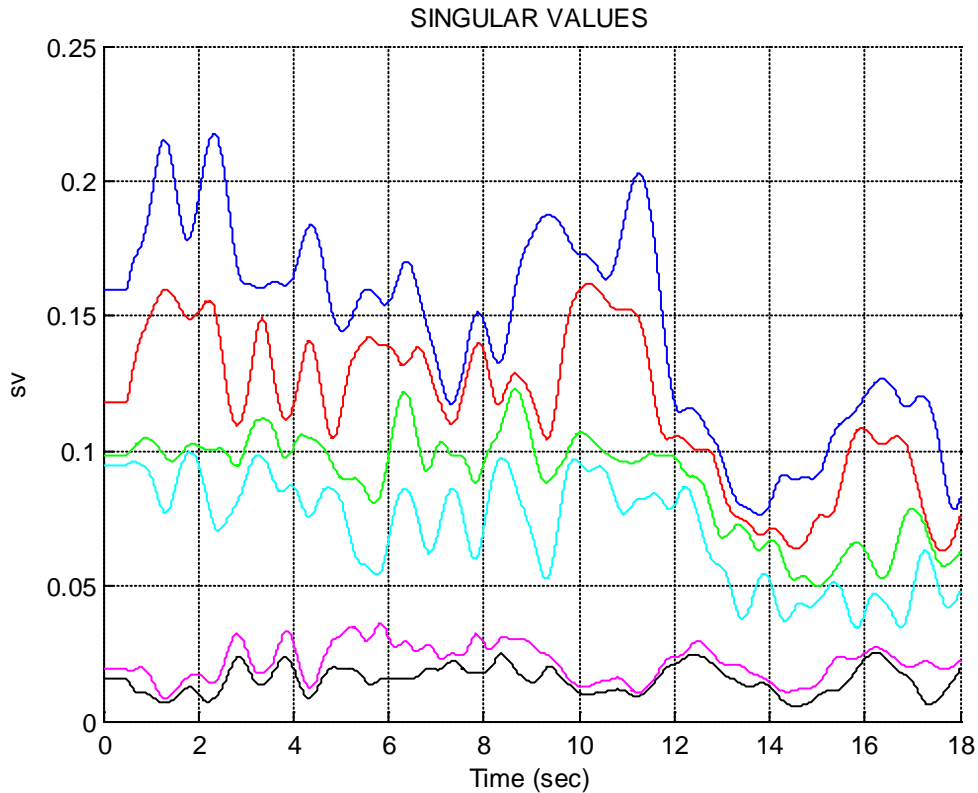
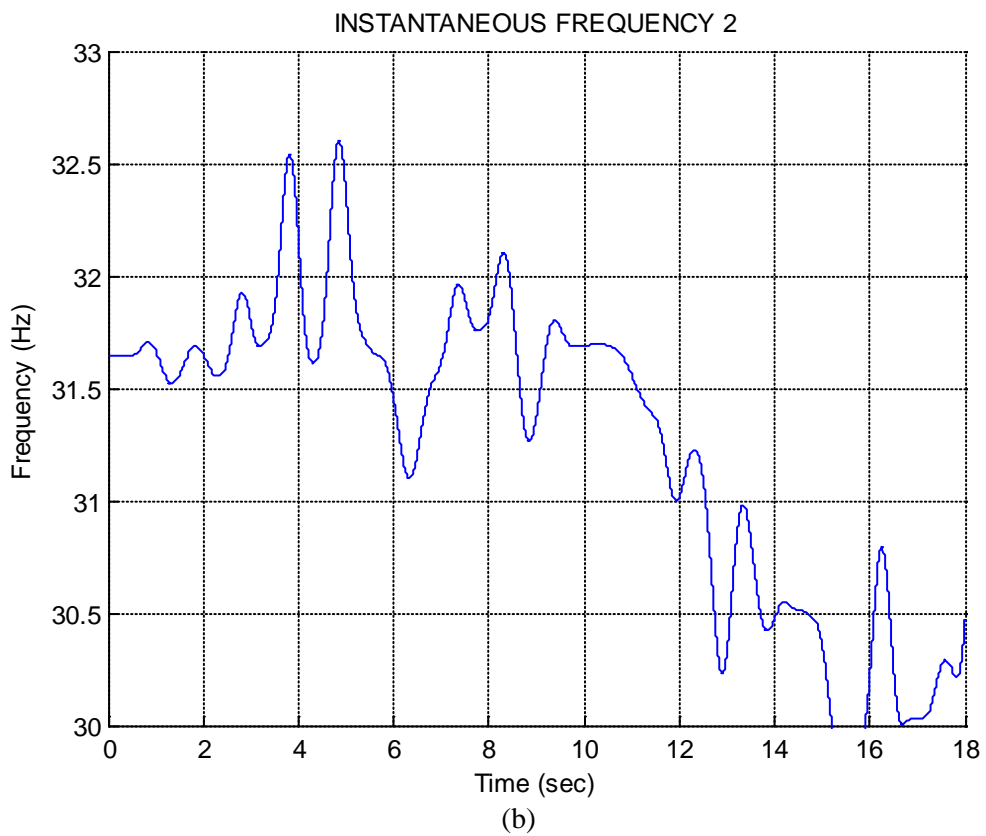
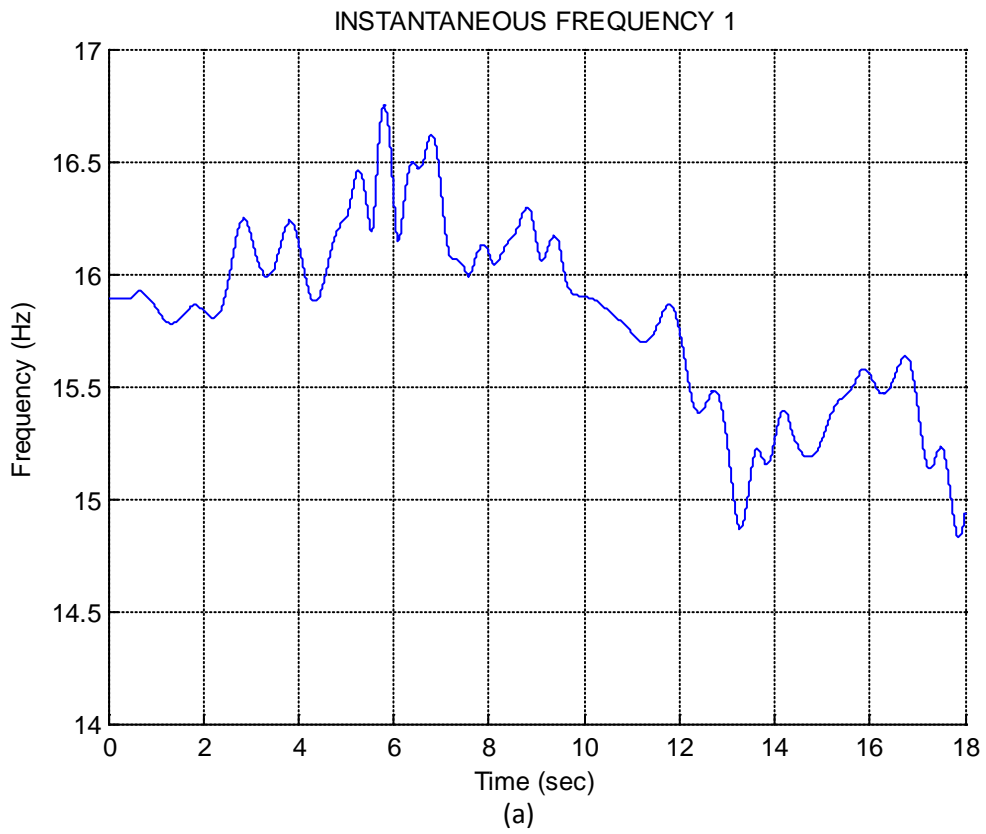


Figure 21. Singular values of the signal used in section 4.2 (Test case 5).



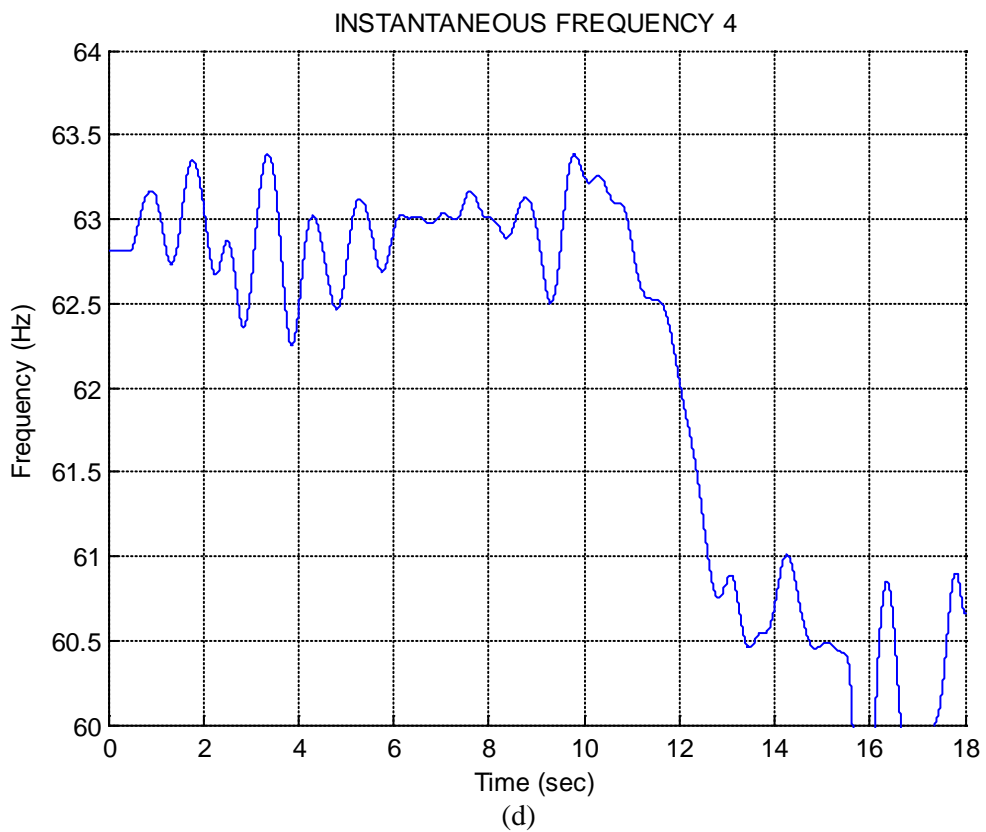
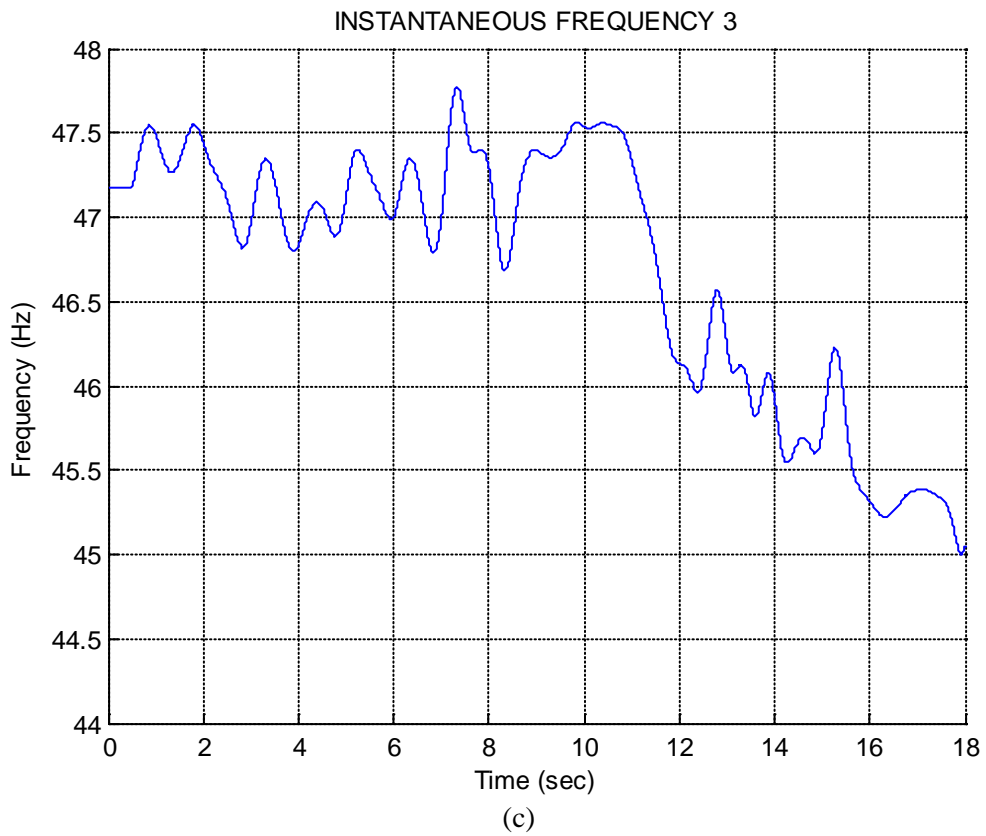


Figure 22. Instantaneous frequencies (a, b, c & d harmonics) for the 6-high rolling mill slow down signal used in section 4.2 (Test case 5).

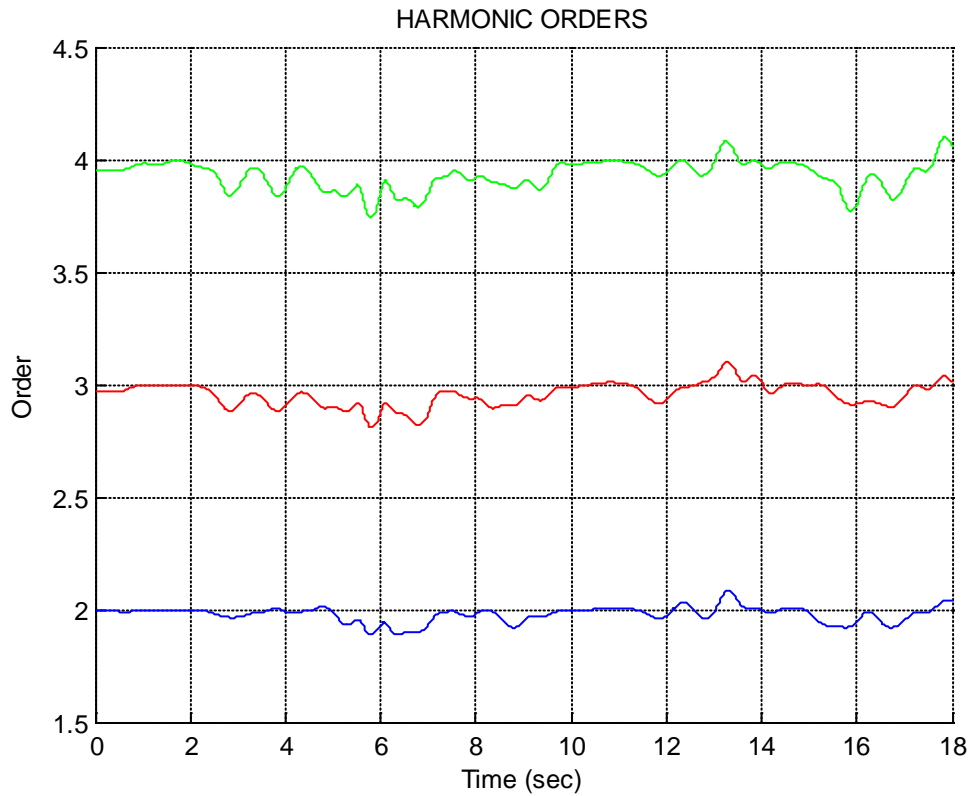


Figure 23. Ratio of second to first, third to first and fourth to first instantaneous frequencies (Harmonic orders) for the 6-high rolling mill slow down signal used in section 4.2 (Test case 5).

5. Conclusion

The proposed IFESIS procedure indicates promising results both in cases of demanding synthetic signals, as well as in cases of experimental and industrial applications, combining effectively the advantages of the Complex Shifted Morlet Wavelets with the advantages of subspace based approaches. Not only the method can accurately recover the instantaneous frequencies, but the non-zero singular values of the corresponding singular value decomposition problem provide an effective means for estimating the number of the harmonic components contained in the signal, an estimate which can be time dependent in signals with a time variable dynamic structure.

Since no specific constraints are imposed on the center frequencies and the bandwidths of the individual wavelets, as well as on the number of wavelets used, a vast number of possibilities is open for the proper selection of an appropriate wavelet structure (possibly iterative and time varying), significantly contributing to the effective application of the method.

Other complementary but critical issues for the implementation of the method, such as appropriate alternative subspace numerical algorithms, alternative estimators of the number of instantaneous frequencies, approaches for calculation of the instantaneous amplitudes and for smoothing the instantaneous frequencies, as well as application oriented specific procedures in several important areas of mechanical signal processing such as condition monitoring, fault detection, conventional and operational modal analysis, etc provide a promising field of open research.

References

- [1] B. Boashash, Estimating and interpreting the instantaneous frequency of a signal—Part 1: Fundamentals, *Proc. IEEE*, vol. 80, 1992, pp. 520-538.
- [2] B. Boashash, Estimating and Interpreting the Instantaneous Frequency of a Signal—Part 2: Algorithms and Applications, *Proc. IEEE* vol. 80, 1992, pp. 540-568.
- [3] K. Rodopoulos, C. Yiakopoulos, I. Antoniadis, A parametric approach for the estimation of the instantaneous speed of rotating machinery, *Mechanical Systems and Signal Processing*, In Press, Corrected Proof, Available online 15 March 2013.
- [4] K.C. Gryllias, I.A. Antoniadis, Estimation of the instantaneous rotation speed using complex shifted Morlet wavelets, *Mechanical Systems and Signal Processing*, 2012, <http://dx.doi.org/10.1016/j.ymsp.2012.06.026> (under press).
- [5] R. O. Schmidt, Multiple emitter location and signal parameter estimation, *IEEE Trans. Antennas Propagation* 34, Mar. 1986, pp. 276-290.
- [6] R. Roy, A. Paulraj, T. Kailath, ESPRIT – a subspace rotation approach to estimation of parameters of cisoids in noise, *IEEE Trans. Acoust. Speech Signal Process.*, vol. 34, Apr. 1986, pp. 1340-1342.
- [7] R. Kumaresan, D. W. Tufts, Estimating the angles of arrival of multiple plane waves, *IEEE Trans. Acoust. Speech Signal Process.* Vol. 34, Apr. 1986, pp. 1340-1342.
- [8] S. G. Mallat and Z. Zhang, Matching pursuits with time-frequency dictionaries, *IEEE Trans. Signal Processing*, Special Issue on Wavelets and Signal Processing, vol. 41, Dec. 1993, pp. 3397-3415.
- [9] A. C. Bovik, P. Maragos and T. F. Quatieri, AM-FM energy detection and separation in noise using multiband energy operators, *IEEE Trans. Signal Processing*, Special Issue on Wavelets and Signal Processing, vol. 41, Dec. 1993, pp. 3245-3265.
- [10] B. Santhanam and P. Maragos, Multicomponent AM-FM demodulation via periodicity-based algebraic separation and energy-based demodulation, *IEEE Trans. Commun.*, vol 48, no. 3, Mar. 2000, pp. 473-490.

- [11] A. G. Poulimenos, S. D. Fassois, Parametric time-domain methods for non-stationary random vibration modeling and analysis – A critical survey and comparison, *Mechanical Systems and Signal Processing*, vol. 20, 2006, pp. 763-816.
- [12] M. D. Spiridonakos, S. D. Fassois, Parametric identification of a time-varying structure based on vector vibration response measurements, *Mechanical Systems and Signal Processing*, vol. 23, 2009, pp. 2029-2048.
- [13] N. E. Huang, Z. Shen, S. R. Long, M. C. Wu, H. H. Shih, Q. Zheng, N.-C. Yen, C. C. Tung, and H. H. Liu, The empirical mode decomposition and the Hilbert spectrum for nonlinear and non-stationary time series analysis, *Proc. R. Soc. London a*, vol. 454, no. 1971, Mar. 1998, pp. 903-995.
- [14] Michael Feldman, Hilbert transform in vibration analysis, *Mechanical Systems and Signal Processing*, vol. 25, 2009, pp. 735-802.
- [15] Francesco Gianfelici, Giorgio Biagetti, Member IEEE, Paolo Crippa, Member IEEE, and Claudio Turchetti, Member IEEE, Multicomponent AM-FM Representations: An Asymptotically Exact Approach, *IEEE Trans. on Audio, Speech and Language processing*, vol. 15, no. 3, Mar. 2007.
- [16] Alexandros Potamianos, Petros Maragos, Speech analysis and synthesis using an AM-FM modulation model, *speech communication*, vol. 28, 1999, pp. 195-209.
- [17] Michael Feldman, Theoretical analysis and comparison of the Hilbert transform decomposition methods, *Mechanical Systems and Signal Processing*, vol. 22, 2008, pp. 509-519.
- [18] Gabriel Rilling and Patrick Flandrin, Fellow, IEEE, One or Two Frequencies? The Empirical Mode Decomposition Answers, *IEEE trans. on signal processing*, vol. 56, no. 1, Jan. 2008.
- [19] Michael Feldman, Analytical basics of the EMD: Two harmonics decomposition, *Mechanical Systems and Signal Processing*, vol. 23, 2009, pp. 2059-2071.
- [20] Thomas F. Quatieri, Senior Member, IEEE, Thomas E. Hanna, and Gerald C. O'Leary, AM-FM Separation Using Auditory-Motivated Filters, *IEEE trans. on speech and audio processing*, vol. 5, no. 5, Sept. 1997.
- [21] N. G. Nikolaou, I.A. Antoniadis, Demodulation of vibration signals generated by defects in rolling element bearings using complex shifted morlet wavelets, *Mechanical Systems and Signal Processing*, vol. 16, 2002, pp. 677-694.
- [22] K. C. Gryllias, I. Antoniadis, A peak energy criterion (P.E.) for the selection of resonance bands in complex shifted morlet wavelets (CSMW) based demodulation of defective rolling element bearings vibration response, *Inter. J. of Wav., Multires. and Inform. Proc.*, vol. 7, 2009, pp. 387-410.
- [23] M.R.Bai, J.Jeng, C.Chan, Adaptive order tracking technique using recursive least-square Algorithm, *Journal of Vibration and Acoustics, Transactions of the ASME*, vol. 124, 2002, pp. 502-511.

[24] M.C.Pan, Y.F.Lin, Further exploitation of Vold-Kalman-filtering order tracking with shaft speed information-I:Theoretical part, numerical implementation and parameter investigations, MSSP, vol. 20, 2006, pp. 1134-1154.